Flexible barriers and trapping of large wood

Ana-Rocio Ceron-Mayo

▶ **To cite this version:**

Ana-Rocio Ceron-Mayo. Flexible barriers and trapping of large wood. [Internship report] ENSE^3. 2020, pp.1-52. hal-03030910

HAL Id: hal-03030910
https://hal.inrae.fr/hal-03030910

Submitted on 30 Nov 2020

HAL is a multi-disciplinary open access archive for the deposit and dissemination of scientific research documents, whether they are published or not. The documents may come from teaching and research institutions in France or abroad, or from public or private research centers.

L'archive ouverte pluridisciplinaire **HAL**, est destinée au dépôt et à la diffusion de documents scientifiques de niveau recherche, publiés ou non, émanant des établissements d'enseignement et de recherche français ou étrangers, des laboratoires publics ou privés.

Distributed under a Creative Commons Attribution 4.0 International License

Flexible barriers and trapping of large wood

Ana Rocío CERÓN MAYO

Master Thesis - Projet de fin d'études
International Master in Hydraulic and Civil Engineering

July 2020

Supervisors: Dr Guillaume PITON & Dr Stéphane LAMBERT
Scholar tutor: Prof. Eric BARTHELEMY

Non-confidential thesis

Acknowledgements

To Guillaume PITON. Thanks for letting me work by your side, for giving me a chance to be part of your research, for teaching me something new every day and showing me how to do the things right. Thank you for all the patience you have in explaining things to me over and over again. I hope one day to have that passion and energy that you devote to everything you do.

To Stéphane LAMBERT. Thank you for giving me the opportunity to collaborate on this internship, for your time and your advice on this report.

To my teachers at ENSE3, especially Eric BARTHELEMY and Fabrice EMERIAULT. The knowledge they share in the courses that they teach, motivates me every day to grow professionally.

To my colleagues at INRAE: Hervé BELLIOT, Alexis BUFFET, Nour CHAHROUR, Fabien DUBOIS, Christian EYMOND GRIS and Marco PIANTINI. Thank you for your help, without you it would not have been possible.

To my parents, Josefina and José Luis, I will never be able to finish thanking you for all the love and unconditional support you have always given me. I love you and I miss you.

To my brothers, Susana and Adrián. I am so proud of you, thank you for your love and patience. I love you.

To my grandmother, my cousins, nieces, uncles and aunts who still look out for me even in the distance.

To my grandfather, who always takes care of me and protects me. I love you, wherever you are.

To my friends in Mexico and France, thank you for your talks, calls, e-mails, messages... In short, thank you for always being present. This work is especially dedicated to one of my best friends, Pedro O. You left early and we lacked more talks and more beers to share, but I thank you for all you shared with me in life, Shine on you crazy diamond.

Finally, to my husband, Miguel MEJÍA. None of this would be possible without you. Thank you for all the patience, for all the support, for all the love, thank you for always teaching me to fight for what I want and never letting me down, thank you for the persistence and wisdom, thank you for accepting me as I am and helping me to grow. After 3 years we are finally achieving our dreams. I love you with all my soul, together forever.

Abstract

The researches published so far on flexible net barriers focused on the control of debris flows and intercepting falling rocks. Few research studies focused on describing the interaction between a flexible barrier and large wood (LW) flows. Due to the limited articles published on this subject, there are a number of issues that have not yet been addressed, which have an effect on the behaviour and design of a net. This knowledge gap is a strong obstacle to the use of these cheap and light structures. Therefore, this research is aimed towards studying some of these: LW-related head losses against flexible barriers and release conditions of LW overtopping flexible barriers.

Several experiments were carried out on a scale model in order to analyze the effect of increasing discharge, as well as the amount of wood volume introduced into the channel, on the water depth at the structure and the eventual release of logs. The flexible barrier was printed on a 3D printer and scale factors were determined so that the barrier deforms consistently with the load it experiences at real scale. Results could then be applied to the prototype scale with more confidence. To the best of our knowledge, this thesis is the first work performed on a scale model of a flexible barrier using a method to rigorously follow the barrier mechanical similitude.

The results revealed that the reliability of flexible barriers as a method of controlling LW flow is quite high. Tests on rigid barriers performed in a previous work showed that overtopping and massive release of LW was nearly systematically observed. Conversely, no overtopping was observed on the same experimental apparatus with flexible barriers: they extremelly permeable and our pumping power was not high enough to submerge them. To find an overtopping condition, it was necessary to place some blockage that favors sufficient increase in water depth and, as a consequence, the release of the LW flow through the dam crest.

With the first series of experiment (without obstruction), a new dimensionless approach for the calculation of head losses based on the ratio between buoyancy and drag force and the dimensionless solid volume of LW was developed and compared with the water depths obtained in the experiments. It showed better performance than different equations that have been proposed for the estimation of head losses related to the interaction of LW and rigid barriers. It was found that these equations over-estimated head losses in flexible barriers. The complementary experiments (with artificial obstruction of the net) enabled to observe seven massive overtopping events. Consistently with the past work on rigid barrier, it was observed that overtopping appear when water level above the net crest is typically about 2-5 times the LW mean diameter.

Contents

Funding: This work was funded by the French Ministry of Environment (Direction Générale de la Prévention des Risques - Ministère de la Transition Ecologique et Solidaire) within the multi-risk agreement SRNH-IRSTEA 2020 (Action *FILTOR*).

Chapter 1

Introduction

1.1 Research context

1.1.1 Project presentation

The material transported by mountain streams, such a sediment and large woods (also called woody debris), from headwaters and hillslopes down to valleys and lowland fluvial systems, can pose a serious hazard in low-lying areas, mainly during extreme runoff events. Several control methods and techniques have been developed over the years to mitigate the adverse effects of this natural process. Among these, the construction of protection structures on streams to trap the material is the most usual (commonly called open check dams). In the last decades, the construction of filtering protection structures for this purpose has increased around the world, the main objective of them is diminishing the flooding intensity (Rossi and Armanini, 2020). However, when the structure is clogged by the presence of large wood, its capacity to reduce the peak of the discharge decreases, aggravating the hazard to downstream areas. Therefore, defining criteria for the design of protection measures is a knowledge gap we must address. In this context, the National Research Institute for Agriculture, Food and Environment (INRAE) is performing a two-years project for the French Environment Ministry to study the interactions between barriers (open check dams) and large wood. By means of a scale laboratory model, the operation of rigid and flexible barriers exposed to the accumulation of large wood is studied. This paper presents only the study on the flexible barrier conducted during the internship. The experiments were carried out at the laboratory of hydraulics at INRAE Grenoble; the experimental set-up consists of a rectangular channel 6.0 m long, 0.4 m wide and 0.4 m high, with an established slope of 2%. A flexible plastic mesh is placed at the channel outlet to simulate the flexible barrier.

1.1.2 INRAE

The Institute

INRAE is a new French public research institution, created in 2020 with the merger of INRA and IRSTEA, two French research institutes that shared interests in the same subjects: agriculture, food and the environment. Under the double supervision of the Ministries of Research and Agriculture, the Institute conducts research, develop innovations, and support public policies with a view to permanently transforming the way we grow crops and breed animals, produce food, and interact with the environment.

Currently, the Institute has 18 research centres and a headquarters (see Figure 1.1), 14 scientific divisions, 268 research and support units, and employs approximately 12,000 people.

ETNA Research Unit

The experimental work is being carried out at the Lyon-Grenoble Auvergne-Rhône-Alpes Centre. The working group is part of the ETNA (Torrent Erosion, Snow and Avalanches) Research Unit, which is based in Grenoble. Its objective is to develop tools applicable to the engineering and prevention of

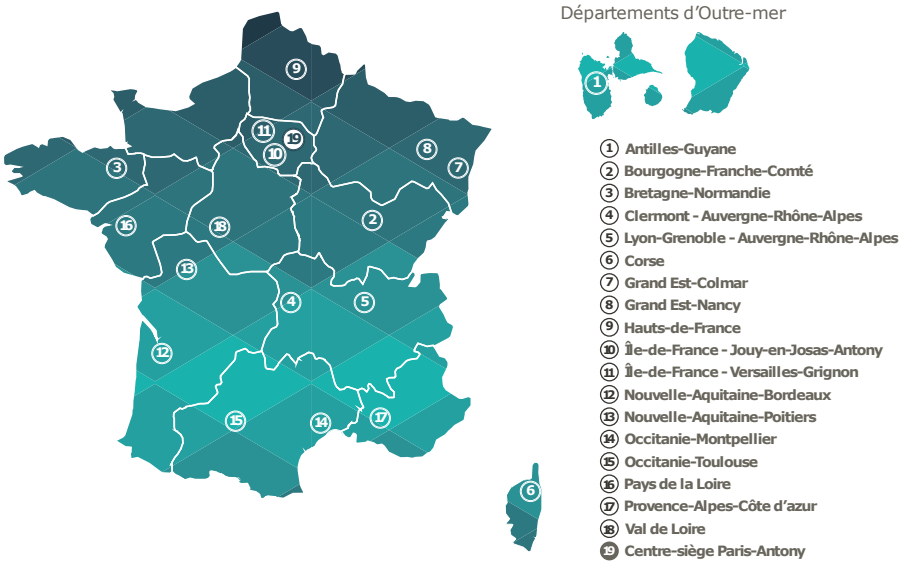

FIGURE 1.1. INRAE research centres.

natural hazards in mountainous areas (avalanches, blowing snow, torrential erosion, debris flows, rock falls, hazards relating to glaciers). It conducts fundamental work in the fields of dynamics of flows and landforms, interactions with elements at risk, protection system design, vulnerability assessment, risk assessment, decision support methodologies and systems in a context of global change.

1.2 Large wood in rivers and flexible barrier current use

Wooden logs are natural elements in fluvial ecosystems, in forested regions mainly, but not exclusively. They reach the river channel through diverse mechanisms such as wind, rainfall, bank erosion, landslide or beavers. Once in the river, they play a major role, in the morphology of the river, but also in the biodiversity. In addition, logs can also represent a hazard for nearby inhabitants and infrastructure, particularly the large ones, hereinafter called "large wood".

The most widely used definition in the literature for a large wood (LW) is a log which exceeds 1.0 m in length and 0.1 m in diameter (Anderson et al., 1978; Keller and Swanson, 1979; Lienkaemper and Swanson, 1987; Wohl et al., 2016). Because of their importance in river corridors, research on LW began in the 1970s, particularly in North America (e.g. Anderson et al., 1978; Keller and Swanson, 1979), and systematically extended to other regions of Asia and Europe (e.g. Harmon and Hua, 1991; Piegay, 1993; Hering et al., 2000).

According to Gurnell et al. (2002), the research on LW has focused on three main themes: flow hydraulics; transfer of mineral and organic sediment; and the geomorphology of river channels. In general, in all these research works it is documented how LW influences and help to keep the health of rivers corridors. Therefore, the challenge is to find the right conditions to maintain the good ecological status of rivers, while minimizing the potential hazard due to LW (Ruiz-Villanueva et al., 2016b).

1.2.1 Environmental perspective

The development of research on wood and its influence on rivers was mainly due to an environmental aspect, linked to the health of salmonid fishes (e.g. James, 1956; Helmers, 1966; Sheridan, 1969). These early studies brought to the light the relevance of this component. LW is an important determinant of habitat structure in river corridors. It stimulates the creation of mesohabitat structures (Andrus et al., 1988; Montgomery et al., 1995; Gurnell and Sweet, 1998). Pools, retention of organic matter and the cover providing by LW are important elements for the development of microhabitats necessary for the feeding, resting and protection of fish and other organisms (Anderson et al., 1978; Braccia and Batzer, 2008; Nagayama et al., 2012). Therefore, rivers with accumulation of LW present a high physical habitat diversity (Ward and Aumen, 1986).

LW accumulations increase water depth, increasing lateral connectivity of the river and floodplains (Brummer et al., 2006) and sustain ponded water in the river channel during drought periods (Dixon et al., 2016). Increased connectivity and overbank flows provide increased resilience for riparian vegetation (Grabowski et al., 2019). Shading provided by this vegetation and the hyporheic exchange flow potentialized by LW reduce water temperature locally (Lautz et al., 2006; Sawyer and Cardenas, 2012). Finally, the presence of LW has been identified as one of the factors that govern carbon input and storage in rivers (Shields et al., 2008), important for the process and fluxes of organic matter.

The loss of wetlands in the last century mainly due to urbanization and agriculture has degraded the ecosystems of the rivers, deteriorating the habitat and diminishing the riparian vegetation (Nagayama et al., 2008). Given the obvious ecological benefits of wood in rivers at various scales, LW are very commonly used in river restoration (e.g. Gerhard and Reich, 2000; Brooks et al., 2006; Dixon et al., 2016; Grabowski et al., 2019) (Figure 1.2). Although most of the restoration cases have reported improvements in the physical habitat, all of them have been short-term evaluations, and long-term results are still lacking, therefore, the technique remains controversial (Roni et al., 2014).

FIGURE 1.2. (a) LW used in a restoration on the lowland River Gade, UK (Grabowski et al., 2019). (b) Installing LW for the restoration on River Washburn (source: https://www.salixrw.com/solution/river-washburn-river-restoration/).

1.2.2 Risk perspective

Hazard associated with LW depends on the volume of wood within a river, and according to Wohl et al. (2016), there are three main hazards to people and infrastructure when wood is present:

- **Mobile wood.** The tree movements in which a log can be found within a channel are: resting, sliding or rolling and floating. These depend on the diameter of the log, the depth of the channel, the resistance and hydrodynamic forces and the characteristics of the wood. Ruiz-Villanueva et al. (2016a) recommend not to use the standard density of wood ($\rho_w = 500$ kg/m^3) to estimate the movement of LW, so they performed a series of experiments where they found that fresh wood has a higher density ($\rho_w = 800$ kg/m^3) than decomposed wood ($\rho_w = 660$ kg/m^3), being the latter the most likely to be transported.

  The movement of the elements in the flow is related to the dimensions of the channel that contains it. If the pieces are smaller than the average width of the channel and narrower than the average depth of the flow, then the probability of movement within the flow will be high (Lienkaemper and Swanson, 1987; Braudrick and Grant, 2000).

  In general, the behavior of the LW within the channel is relatively stable and quiet. This equilibrium is broken once high floods occur (which are rare) and facilitate the transport and recruitment of wood, becoming a potential danger and creating damage in the surroundings, as well as in the upstream and downstream areas of the channel, figure (1.3a).

- **Altered movement of sediment and patterns of erosion and deposition.** When there is a perturbation in the flow of a river, the velocity of flow changes and as a consequence the

transport of sediments as well. The effect of LW flow within a river with respect to sediments is the change in sediment dynamics, ranging from deposition, erosion, scour, which together or individually, can cause significant damage to the channel that transports them or to existing structures in the river, (figure 1.3b). This source of diversity in wild areas must sometimes be prevented near human assets

- **Increased flood stage**. Once the LW is floating in the channel, the increase in the amount of these can cause obstructions and, in many cases, induce the water level to rise. Among the possible consequences of the change in level, there is a risk of possible flooding in areas surrounding the channel. As LW accumulates against bridges, deviated flows can cause damage in the floodplain.

FIGURE 1.3. (a)LW transport (source: https://energisch.ch/); (b)LW accumulation at a bridge (source: https://eu.desmoinesregister.com/)

1.2.3 Solid transport processes

Large Wood flow

Even though there are several definitions of large wood flow and woody debris, within this research it was decided to use the term LW to define the mixture of wood elements (logs), fine material FM composed mainly of branches and vegetation and eventual sediments (small rocks).

Based on experiments conducted by Braudrick et al. (1997) where the transport of floating logs in a gravel-bed river was simulated to analyze the behavior and accommodation of the floating elements, it is possible to find three different ways of transport based on the interaction of the components: (i)Uncongested: There is no contact between the logs, they move independently, (ii) Congested: For this condition, the assembly of several logs behaves as a unit, that is, there is an interaction between the logs and the movement of one log affects other elements within the grouping, (iii) Semi-congested: Represents a combination between the uncongested and congested cases, where there are loose elements and elements as a whole.

Figure 1.4a shows the arrangements that have been detailed for the transport of LW. This illustration was taken from the investigation made by Ruiz-Villanueva et al. (2019), which added the term *hypercongested* to the three existing transport regimes and described it, as a mass that usually covers the entire width of the channel that contains it and where most of the logs that compose it have a direction perpendicular to the flow, moving and having contact with other logs generating a pivot effect in the mass.

There are also two types of hypercongested flow, both occurring in the front section of the LW flow: (i) Dry, where the water level is lower than the LW flow depth which means that the logs don't float and are only found rolling or sliding on the river bed, (ii) Wetted, there is a water surge behind the front of the LW flow where the water level h is higher than the wood flow depth, allowing the logs to float, it is composed of a large mass of logs able to rotate, move and function as pivots.

With the help of a ternary diagram (see Figure 1.4b), it is possible to find and classify the type of LW regime. Then, for this investigation a **congested** regime will be studied.

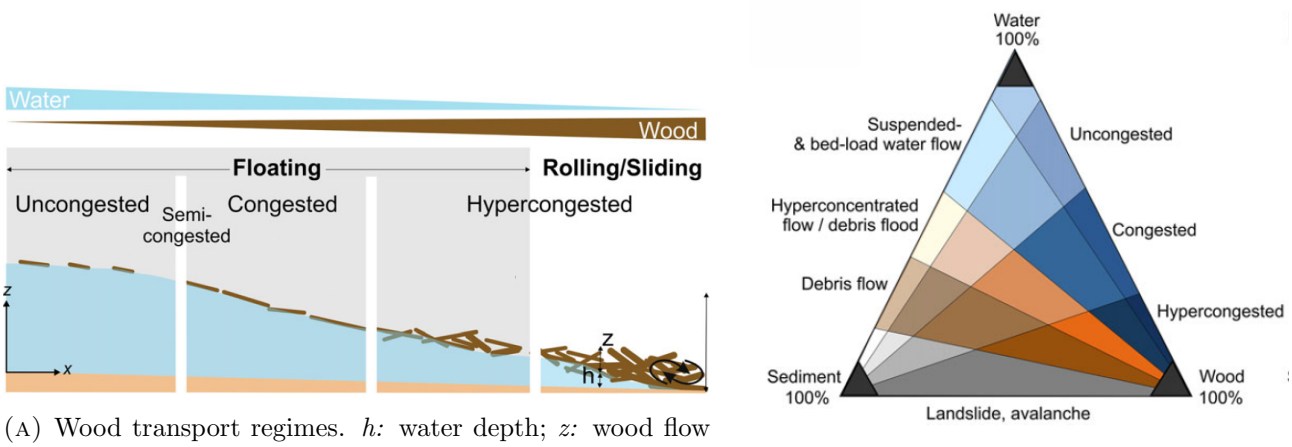

(A) Wood transport regimes. *h:* water depth; *z:* wood flow depth.

(B) Ternary diagram of sediment-water-wood.

FIGURE 1.4. Large wood flow regimes (source: Ruiz-Villanueva et al., 2019)

Debris Flows

Another solid transport process that is sometimes related to LW and torrential hazards are debris flow. There are many researches on debris flow describing its composition, behavior and mitigation measures for when it occurs. Even though the main topic of the present report is not debris flow, it is important to mention it in order to differentiate it from woody debris and to identify the structures that are used to control it and therefore reduce the damage it causes. It is worth mentioning that flexible barriers have been mostly used to protect against debris flows rather than LW flow so far.

According to Brighenti et al. (2013), debris flow is a phenomenon that occurs suddenly in the form of landslides or erosion with rapid velocities (typically 1-10 m/s) at the front. It is the result of a combination of grain, water and air (and sometimes also includes vegetation) and is linked to extreme weather events (rain, rapid snow melt). The flow has an unstable and not uniform behavior, with a high energy load allowing a long propagation inside and outside of the channel that contains it, causing then, more destruction in its path (figure 1.5a).

Like many natural events, debris flow is a difficult phenomenon to study and to predict due to the lack of historical data as well as its short duration. However, for several years, many researchers have dedicated time and effort to characterize it, which has allowed them to propose structures for damage reduction in the presence of this phenomenon, (figure 1.5b).

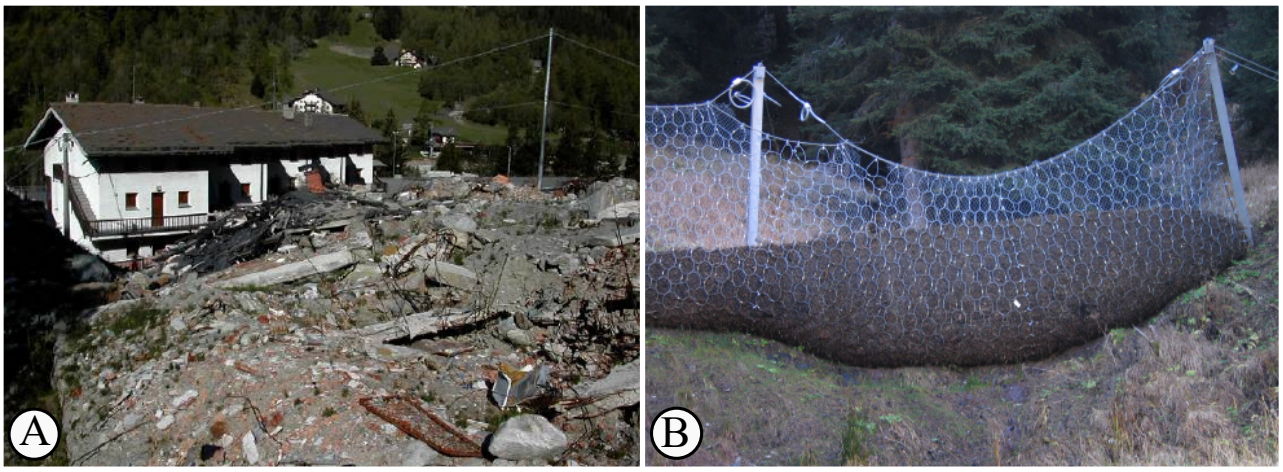

FIGURE 1.5. (a) Debris Flow deposit, (b) Filled flexible barrier system. (Wendeler et al., 2007)

1.3 Objectives of the thesis

The objectives of this experimental study are to determine how large wood increase head losses in a flexible barrier and for which conditions large wood overtop the barrier and are released downstream. This research corresponds to a continuation of the analysis that Piton et al. (2020) carried out to obtain the results of the objectives already mentioned, but applied to a rigid barrier.

This thesis consists of five chapters:

Description of the characteristics of the main topic of this research was provided in this Introduction: the Large Wood (LW) flow. It describes the risks and benefits that this phenomenon has in nature and in the environment where it occurs.

Chapter 2 identifies some types of barriers used for the control of LW flow and the characteristics that they must fulfill. Flexible barriers are emphasized and criteria for functional and structural design are described for both LW flow and debris flow. In addition, some investigations that have been made to calculate head losses related to LW are referred to.

Chapter 3 is an explanation of the parameters, instrumentation and experiments that were carried out in order to achieve the research objectives. Summary explanations of the points needed to work with models and prototypes are provided. It is important to mention that the scale model as well as the prototype, do not represent any particular site. The materials, dimensions and configuration used in the experiments were chosen in order to test the efficiency and strength of the flexible barriers trapping LW.

The results of the experiments mentioned in Chapter 3 are shown in Chapter 4.

Finally, Chapter 5 presents the conclusions reached, as well as a perspective on the possible areas of opportunity for further development in the control of LW flow.

A list of symbol is provided before the reference list

Additionally, there is an appendix showing the computation of the net height. The methodology for determining the net height is based on the research done by Rimböck (2004) and is only attached as an example, because the results of the calculations were not used within this research. Also, other appendices show the measurements of the experiments and some photos corresponding to some experiments.

Chapter 2

Large wood trapping structures

2.1 Rigid barriers

2.1.1 Sabo works and torrent control

According to Walter C. Lowdermilk (Water Resources and Related Land Use in Japan): "Sabo[1] is an apt Japanese term first used in the law of 1889 to designate works of check dams in stream channels and revegetation of eroding slopes as related and supplementary activities". During the IAHS (International Association of Hydrological Sciences) General Assembly in Bruxelles in 1951, the term "Sabo Works" was proposed proposed such works for torrent and mountain stream control.

Sabo works are constructed upstream of a devastated torrent at a site where sediment production and discharge is especially large. They store sediments, which runs down from the upstream, in order to reduce the discharge downstream and also prevent the outflow of unstable sediment deposited at the bed of a torrent (Chanson, 2004b).

When a sabo dam stores sediment up to its capacity, the river width is widened with the resulting effects of creating a gentler torrent bed gradient and weakening the potential force of sediment flow or running water, preventing the collapse of the river banks.

A sabo dam is also capable of preventing sediment disasters by means of temporarily storing sediment to reduce the volume of sediment outflow downstream. Landslides on vegetated hillslope being particularly common in Japan during typhoons, Japanese sabo engineers developped a great expertise in the design of LW traps using steel tubular structures (Chanson, 2004b; Horiguchi et al., 2015).

In Europe, sabo engineering is referred to "torrent control" and sabo dam to "(open) check dams" or "barriers" (Piton et al., 2017). From the perspective of Piton and Recking (2016), open check dams are mostly dedicated to manage sediment transport but some structures are specifically intended to LW, which are categorized as:

- **Light structures** are structures widely open (Figure 2.1). Piton and Recking (2016) describe the sectional dams as open structures where the space between the elements that make them up is larger than half the height and width of those elements, in order to reduce the flow and consequently the risk of flooding. This type of dam is mainly made up of piles, however, it is possible to find that some are made up of fins.

  As mentioned above, the term SABO dam refers to open check dams. In the research carried out by Chanson (2004b), it is possible to find several structures that can be considered as such, however, in this section we will only talk about those that qualify as light structures: tubular grid dams (Figure 2.1b). As the name implies, this type of dam is a rack formed by large tubes whose diameters vary between 0.5 and 1 m, and whose main objective (due to its porosity) is to catch as many big elements as possible (big logs, boulders).

  The piles can be directly drilled in sediment (Figure 2.1a) or be equipped with a foundation made of reinforced concrete (Figure 2.1b). There are also different ways of accommodating the

[1] Japanese meaning: SA(sand) BO(prevention)

elements, giving place to different shapes, some of which are V-shape (Figure 2.1a), Λ-shape and straight shape (Figure 2.1b), where the main reason for choosing between these is the need to increase the discharge capacity of the dam which is proportional to the total length of the dam.

FIGURE 2.1. Light structures: (a) V-shape sectional dam made with piles (Ruiz-Villanueva et al., 2016b); (b) SABO dam tubular (Chanson, 2004b)

Once the transport of wood occurs, they begin to pile up themselves between the piles in such a way that they create a "new dam" that functions as a trap for other sediments. According to the research carried out by Schalko (2018), when exists a light barrier capable of retaining LW one of the possible consequences is the formation of a blockage by accumulation in the cross section, which tends to adopt a trapezoidal or triangular shape (figure 2.2). If the flow and logging continues, the LW then begins to form an "LW carpet" on the surface of the channel.

FIGURE 2.2. Model large wood accumulation at a retention rack with a movable bed, taken from Schalko (2018)

.

The high permeability of these structures enable low impact, i.e. low trapping, on low magnitude floods. This, combined with the ease and low cost of maintenance, are benefits desired when considering these types of dams. To avoid possible overtopping when the peak discharge of one hydrograph is reached, it is recommended good maintenance and continuous cleaning, and regarding to the design of this type of structure it is necessary to consider a high enough crest.

- **Heavy structures** are conversely less permeable with a large dam body though, increasingly equipped with a couple of large openings. The research carried out by Armanini et al. (1991), has made it possible to define more precisely the term as well as the purpose of open check dams. Armanini's work represents a guideline for the classification of the different structures:

  (i) Slit-dam: Structures designed with one or more vertical openings which, during minor floods, are intended to allow continuous transport of sediments in order to maintain an upstream volume capable of generating self-cleaning of the structure.

(ii) Beam-dam: Structures designed with one or more horizontal holes, where the size of the holes depends on the size of the elements to be retained.Heavy structures have been studied by other author, see Piton et al. (2020)

2.1.2 Head losses at light barriers

As previously mentioned, one of the main consequences of the obstruction of rigid barriers, is the backwater rise as a result of the accumulation of LW. Several authors have dedicated their research to address this event, among which we highlight:

- The research done by Schmocker and Hager (2013) focused on scale models, and the parameters on which they concentrated were the accumulation of LW flow and the backwater rise. The results of their research showed that the approach-flow Froude number on the debris accumulation process plays an important role in the backwater rise, unlike the properties of the LW flow that were insignificant in the analysis. They proposed a simple equation adjusted on experiments with LW accumulated against a dam made of piles:

$$\frac{\Delta h}{h_0} = 0.4 + 1.9Fr_0 \tag{2.1}$$

  with Δh the head loss (m), h_0 the water depth without LW (m) and Fr_0 the Froude Number of the flow without LW. Equation 2.1 can be rearranged and adjusted it in order to compute the water depth with LW, h:

$$h = h_0 + \Delta h = h_0 \left(1 + \frac{\Delta h}{h_0}\right) = h_0(1.4 + 1.9Fr_0) \tag{2.2}$$

- Schalko et al. (2019a) investigated the backwater rise caused by spanwise LW accumulations with a movable bed, in a scale model and with a dam made of piles. The results are outlined in design equations that allow to estimate the effect of LW volume on the backwater rise. In their investigations, they proposed:

$$\frac{\Delta h}{h_0} = 5.4 f_A \frac{Fr_0(V_s/(h_0 b_C \phi_{LW,m}))^{1/3}(9FM + 1)}{a} \tag{2.3}$$

  with Δh the head loss (m), h_0 the water depth without LW (m), Fr_0 is the Froude Number of the flow without LW, V_s is the solid LW volume (m^3), b_C is the channel width (m), $\phi_{LW,m}$ is the mean log diameter of the wood (m), FM is the fine material added as a percentage of V_s (%) and a is defined as a bulk factor corresponding to the compactness of an accumulation (-), f_A is the accumulation type factor that helps to take into account the natural LW accumulation and the movable bed, then: $f_A = 1.00$, for predefined accumulation; $f_A = 0.55$, for natural accumulation with a fixed bed and $f_A = 0.30$, for natural accumulation with a movable bed.

  The compactness factor a can be approximated:

$$a \approx (5 - 1.35Fr_0) \tag{2.4}$$

  Then, to compute h, one can rearrange and merge equations 2.3 and 2.4:

$$h = h_0 + \Delta h = h_0 \left(1 + \frac{\Delta h}{h_0}\right) = h_0 \left(1 + 5.4 f_A \frac{Fr_0(V_s/(h_0 b_C \phi_{LW,m}))^{1/3}(9FM + 1)}{5 - 1.35Fr_0}\right) \tag{2.5}$$

- Piton et al. (2020) performed a series of experiments on different dams (trapezoidal, slit, slot and SABO dam) in order to provide an experimental quantification of LW-related energy dissipation. Their research also focuses on calculating the increase in water level due to the interaction of the dam and the LW flow, taking into account the capacity of flow through its open body and above

the spillway. In their research, they use β=$\Delta h/h_0$ to address LW-related energy dissipation. Then, to calculate h:

$$h = h_0 + \Delta h = h_0 \left(1 + \frac{\Delta h}{h_0}\right) \Leftrightarrow h_0 = \frac{h}{(1+\beta)} \tag{2.6}$$

They adapted the rectangular weir equation:

$$Q = \frac{2}{3}\mu b_w \sqrt{2gH^3} \tag{2.7}$$

where μ is the weir coefficient, b_w is the spillway horizontal width (m), H is the hydraulic head (m). We know that H=$h + u^2/2g$=$h(1 + Fr_0^2)$, with u is the flow velocity (m/s), thus the second and third forms of equation 2.7, introducing eq. 2.6:

$$Q = \frac{2}{3}\mu b_w \sqrt{2g\left[h_0\left(1 + \frac{Fr_0^2}{2}\right)\right]^3} = \frac{2}{3}\mu b_w \sqrt{2g\left[\frac{h}{(1+\beta)}\left(1 + \frac{Fr_0^2}{2}\right)\right]^3} \tag{2.8}$$

If there is no LW inside the channel, then $\beta = 0$ and the equation will return to its usual setup. If for example $\beta = 0.5$ is set, it means that the water level will increase by 50% compared to the pure water flow, in order to in order to convey the same water through the accumulation of LW.

2.1.3 Release condition in open check dams.

According to Furlan (2019), when ratio between the overtopping depth and the log diameter becomes higher than two, the probability that logs be released over spillways of reservoir dams is high. Consistently, in the research realized by Piton et al. (2020) on rigid barriers, some dimensionless numbers were used to define the conditions of the flow and the environment in which the release of LW occurs, that is, when the barrier loses its trapping capacity. The dimensionless overtopping depth h^* proved to be relevant:

$$h^* = \frac{h - z_2}{\phi_{LW,m}} \tag{2.9}$$

with z_2 as the crest level of the flexible barrier (m).

In the application of this equation to several dams, Piton concludes that the maximum length of the LW plays a secondary role in SABO dams.

This approach and the and the ones mentioned above (Schmocker and Hager, 2013; Schalko et al., 2019a) will be tested on flexible barrier conditions.

2.2 Flexible barriers

Recently and thanks to its simplicity to be installed thus to the low impact on the environment that they generate in the vicinity of the place where it is located, the use of flexible net barriers has been amplified throughout the world. The flexible net barriers are simple and light structures (see figure 2.3), whose main components are:

- A net usually formed by rings.
- Horizontal and vertical cables anchored to the sides of the channel, in order to support the net.
- In the case that the net are very wide, posts anchored to the ground are used.
- The use of energy dissipaters is mainly associated with rockfall, however, they can also be used for debris flows and LW flows.

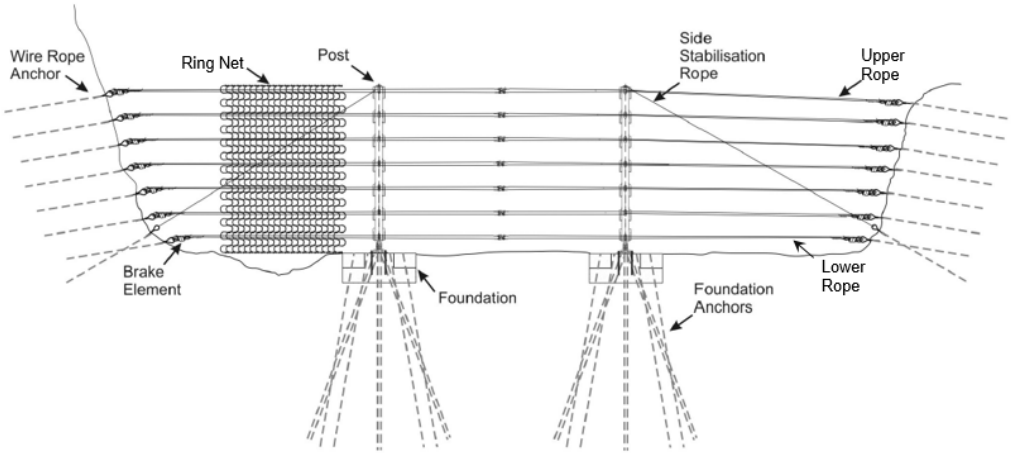

FIGURE 2.3. Flexible barriers scheme (Adapted from Bichler et al., 2012)

The material of the net and cables, the diameter and shape of the rings, the quantity and diameter of the cables to be used, as well as the location of these, are parameters that will be discussed later.

In the following both functional and structural design criteria for flexible barriers are reviewed. Functional design aims at determining the features of the structure required for it to achieve its function (i.e., trapping LW ou debris flows), e.g., location, height, bottom clearance, mesh opening. Conversely, structural design aims at determining the mechanical features of the structure such that it will resist the loads expected during its lifecycle.

2.2.1 Functional design criteria

Functional design for LW flexible barriers

For the design of a net, Rimböck (2004) considered a number of factors necessary to obtain a properly and efficiently functioning net. In order to facilitate the calculation of the net height, only some of all the parameters mentioned by Rimböck (2004) in his research will be used in this investigation (Table 2.1). Rimböck (2004) also provides a graph (see Figure 2.4) that allows to determine the appropriate structure to use against the LW, according to the amount of wood and the discharge.

TABLE 2.1. Limits of the factors applied in a flexible barrier.

Channel width b_C (m)	Unit Discharge $q = Q/b_C$ (m^3/sm)	Solid volume of LW V_S/b_C (m^3/m)	Slope S_0 (%)
≤ 15	≤ 5	≤ 20	≤ 5

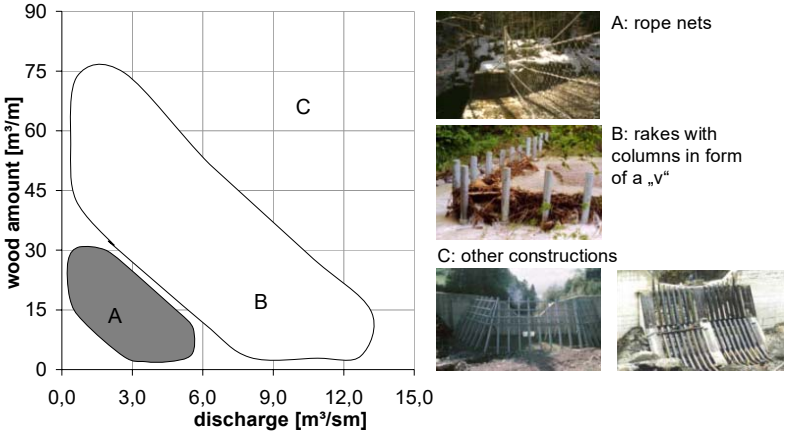

FIGURE 2.4. Application range of various large wood trapping structures according to Rimböck (2004) depending on unit discharge and unit large wood volume

Then, as an example, if it is known that the unit discharge in a channel is $q = 3m^2/s$ and the wood content for it ranges from $1 - 20m^3/m$, the most suitable option for the control of LW flow in the channel is a flexible barrier.

- **Barrier location** Regarding the location of the flexible barrier, it is recommendable to do it in a place where the slope of the channel is not higher than 5%, and as mentioned above, in an almost straight section. It is also recommended that both the margins and the channel bed be paved upstream and downstream (with respect to the net), with a length of at least twice the backwater level.

- **Crest level, z_2.** It is the essential parameter that refers to the height of the net that will be used and installed in the site. This height will define the trapping volume capacity and must be high enough so that an overtopping condition is not generated, i.e. release of one or more logs above the net.

  So the crest elevation z_2 (m) should be higher than the water depth which can also be rewritten with initial water depth h_0 (m) and headloss Δh (m) by:

  $$z_2 = h + f = h_0 + \Delta h + f \tag{2.10}$$

  with h total water depth (m), f freeboard (m).

  The only guidelines about computing flexible barrier height was published by Rimböck (2004). He proposed to compute h using:

  $$h = 4.44 \left(\frac{V_S}{b_C}\right)^c \cdot FM^{0.17} \cdot \left(1 - \frac{35 - K}{105}\right) \cdot \sqrt{\frac{Q}{3b_B}} \tag{2.11}$$

  with V_S is the total solid volume of Large Wood (m^3), b_C is the width of the channel (m), b_B is the width of the barrier (m), FM is the percentage of fine material contained in the total volume of large wood (%), K is the Strickler coefficient of the bed channel ($m^{1/3}/s$), Q is the total water discharge (m^3/s) and, c (-) is a function of the slope of the channel S_0 ($c = 0.20$, for $S_0 = 1.0\%$; $c = 0.25$, for $S_0 = 3.0\%$; $c = 0.26$, for $S_0 = 5.0\%$; with the possibility of interpolating other numbers). On Appendix A, an example of this framework is provided with step by step calculations that were made to size the flexible barrier using equation (2.11).

  Eq. (2.11) was supposedly developed on a scaled model and then probably tested on a prototype. In the experiments made by Rimböck and Strobl (2002) in the prototype, it is mentioned that these were performed with a unitary discharge Q/b_C=3 m^3/s, then it is assumed that they proposed the last term of the equation with the square root to extrapolate for other unit discharge. Also in the same investigation it was specified that the percentage of fine material considered was $FM = 15\%$, while the roughness had a value of K=35 $m^{1/3}/s$.

  To the best of our knowledge, Eq. (2.11) has not been cross-controlled with other experiment or field measurement. No recommendation on freeboard was given by Rimböck (2004).

- **Mesh opening** Although mesh size is not a fundamental parameter to calculate, Rimböck (2004) recommends using diameters close to 0.30 m for small flexible barriers and 0.50 m for flexible barriers with 7 meters or more in height.

- **Bottom clearance, z_1.** This distance corresponds to the space between the lowest rope and the bottom of the channel where it will be installed. It is of utmost importance and must be carefully determined considering that, if the distance is small, the barrier will fill up quickly because the trapping process will start rapidly (mainly with fine elements). On the contrary, if the distance is very large then the functionality of the net will be null and will allow the passage of large logs to the downstream.

  One way to find this value, is to consider the flow depth at which a significant transport of logs begins. Rimböck (2004) points out that a good parameter to obtain this value is to consider the

flow depth of a flood of 5 to 20 years, and if it is not known, to assume a distance of 0.5 to 1.0 meters.

Once the trapping process begins, the net will be deformed horizontally and vertically so this can increase the bottom clearance. If this is to be prevented, it will be necessary to put some intermediate posts, which are designed against impact forces and with a vertical component.

- **Fixed bed level.** Rimböck (2004) recalls that the bed level should be fixed by a structure otherwise scouring will occur under the barrier. Schalko et al. (2019a,b) studied this process on light rigid barrier. They concluded that the scouring can be quite deep and that the headloss might decrease by 45%-70% (see f_A factor in eq. 2.3). Their structure was not equipped with a bottom clearance so the eventual release of LW below a scoured structure was never been studied.

- **Channel cross section shape.** Regarding the geometry of the channel, it is important to mention that in a channel whose margins are mild slope, the LW flow will have more space to expand and its accommodation will be easy, so the water level will not rise much (Figure 2.5 left panel). In addition, the force with which the LW affects the net can be less if the banks and the bottom of the channel are rough. However, once the pieces of wood begin to pile up on the rocks located on the banks, they can cause erosion and rearrangement of the rocks, thus stopping the friction forces (Figure 2.5 right panel).

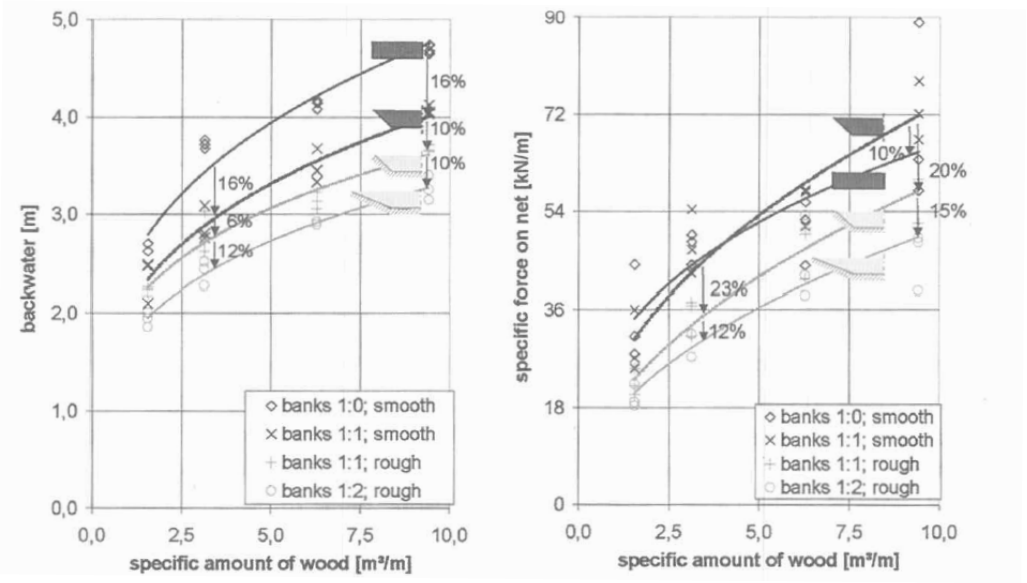

FIGURE 2.5. Effect of roughness and bank slope on water level rise (Left). Effect of roughness and bank slope on impact force on the net (Right). (Rimböck and Strobl, 2002)

Functional design for debris flow flexible barriers

Normally, debris flows are characterized based on their density, flow speed, flow height, total volume, diameter of single elements, channel slope and sediment angle (Volkwein, 2014). All of these parameters influence the design of the net: the front density (grain size distribution and the water content), the height and the flow velocity participate in the pressure applied to the net, while the total volume, the channel slope and the sediment angle help determine the containment capacity of the barrier.

Since the main topic of this research is not debris flow, but LW flow, only some important recommendations will be mentioned to be taken into account when designing a flexible barrier against debris flow.

- **Crest level and shape** The crest level is simply fix to achieve a given storage volume. The use of wing cables is recommended for the control of erosion at the margins and to ensure that the debris flow is concentrated towards the center of the flexible barrier. These should be attached

to the last cable (the upper) with a clamp and should form an angle of approximately 30° to the plane of the net.

- **Mesh Size.** One of the main functions of a flexible debris flow barrier, in addition to control and mitigation, is to absorb the dynamic pressure exerted by the debris flow and then transfer the impact and compression forces to the supporting structures (ropes) and then to the anchors. However, nets can function as a dewatering mechanism, i.e. dehydration of the debris flow to promote deposition of coarse grains and only drain water and small particles. Therefore, the mesh size should be approximately equal to the particle size d_{90}, i.e. 90% of the mass of the flow is composed of particles with a diameter smaller than this value. The width thus be clogged only if boulders are transported and let water flow pass.

- **Bottom clearance.** As with LW flow, for the flexible barrier to meet the objective of controlling debris flow and then begin to fill the space for volume storage not too soon , there must be a correlation between debris flow height and bottom clearance.

  According to Wendeler (2016), in order that blockage of material occurs and the sediments start to accumulate thereby favoring the vertical filling of the barrier, the distance that must exist between the bottom of the channel and the bottom of the barrier is:

$$z_1 < 2/3 h_{DF} \tag{2.12}$$

  with z_1, the distance between the bottom of the channel and the first support cable (the lowest) (m) and h_{DF}, flow depth of the debris flow(m). The opening must be carefully calculated because if z_1 is very close to $2/3 h_{DF}$ or exceeds this value, then the debris flow will pass through it causing a late blockage and diminishing the function of the flexible barrier. On the other hand, if the opening is very small, the blockage will be fast and therefore the flexible barrier will fill up quickly as well as the reservoir.

  The channel bed also plays an important role in the correct functioning of bottom clearance. Soil erosion can occur if the bed is made of loose material, increasing the distance between the barrier and the bottom of the channel. It is recommended that the bedding material be made of solid rock.

2.2.2 Structural design criteria

Structural design for LW flexible barriers

Rimböck and Strobl (2002) and Rimböck (2004) carried out a series of experiments in a model test and in a full scale-nature test, in order to find the acting loads in a net due to LW flow. These are some of the conclusions that they made after comparing the results in both tests:

- The cables represent a fundamental part within the flexible barrier, specifically the intermediate and upper ones. They are the main elements that support the load, each one is capable of transmitting 60% of the total load to the elements to which they are anchored. Hence, the importance of assigning an appropriate diameter, which can vary between 18 and 28 mm.

  Within the flexible net, the bottom cable is also important because of the high loads it is exposed to. Therefore, it is recommended to pay attention to the choice of the distance between the bottom of the channel and the cable.

- The dynamic force, the one that occurs in kinetic energy when a log impacts a cable and is later transformed into the potential energy of the elastic strained rope, is not fundamental to design a cable (unless high speeds or debris flow occur). The high headlosses related to LW trapping rapidly reduce upstream velocities and associated impact forces. The rings of the net absorb most of the impact energy (more than 85%) therefore, the use of these is recommended. Before clogging occurs, a single trunk may hit the net. Even if a ring breaks, the net will not lose or diminish its effectiveness.

- If the LW flow is delivered in a congested or hyper-congested regime, the mass of logs will absorb the greatest amount of energy thus decreasing the dynamic forces during the trapping process.
- Anchors should be installed with an angle between 10° and 20° from the plane of the net.

Structural design for debris flow barriers

Wendeler (2016) propose some recommendations for the structural design of a flexible barrier as a mitigation measure for debris flows. The following are some of them, based on the main components of a flexible barrier (Figure 2.3):

- As in the LW flow, the cables are the main elements in charge of supporting and transmitting the forces applied by the debris flow on the net. It is recommended that these be rounds with diameters of approximately 22-28 mm
- The brake elements have been used mainly in flexible barriers designed against the impact of falling rocks. The use of these is highly suggested to provide more length to the cables to which a clamp attaches them; and they absorb energy through plastic deformation and friction in the clamp.
- The anchors represent a fundamental element for the optimal functioning of the flexible barrier. The flexible anchor head is responsible for supporting the loads on the cables transmitted to the mesh when the debris flow load occurs. The anchor length may vary from 2 to 10m, according to the load-bearing capacity of the soil, so it is advisable to provide a foundation for the anchors. In addition, the anchor arrangement should be chosen based on the geometry and dimensions of the barrier.
- Although the design and purpose of a flexible barrier is to control the debris flow, it will face an overflow if another surge occrus. This occurs when the system is full, either because of maintenance or because it was designed for this purpose (Multi-level debris flow barriers). Consequently, it is strongly advised that both the wing cable and the cable to which it is attached (the upper one) have an abrasion system capable of resisting the impact of large blocks. Since the abrasion system will be in contact with the shearing and the additional load of the overflowing, it has to comply with specific parameters in terms of robustness.

2.2.3 Additional references useful on LW and flexible barriers

There are several and numerous studies on debris flow and large woods, so Table 2.2 shows a brief summary of some of them that I consider important and useful.

Table 2.2. Important references on large wood and flexible barriers.

Topic	Reference	Information contained
Large Wood	Bocchiola et al. (2008)	Channel experiments to characterize the movement and accumulation of LW in rivers.
	Comiti et al. (2016)	Link between the volume of wood moved in a flood and the area of the basin.
	Hashimoto et al. (2016).	Experiments in channels to see the wood log behaviour in debris flow on an open chek dam.
	Wohl et al. (2016)	Overview of knowledge gaps related to wood recruitment, transport, storage and the manner how beavers affect LW dynamics.
	De Cicco et al. (2018)	Interaction of the LW with bridges in a channel.
	Addy and Wilkinson (2019)	Selection and brief description of some research done with models to predict benefits and consequences of LW in channels.
	Grabowski et al. (2019)	Overview of improvements made on the benefit and risks associated with the use of wood for river restoration and management.
Flexible barriers	DeNatale et al. (1999)	Study of the relationship between accumulation and distribution of debris flow in a flexible barrier.
	Roth et al. (2010)	Application of FARO software to represent the dynamic response of the flexible barrier due to debris flow.
	Canelli et al. (2012)	Rigid and flexible barriers were compared to evaluate the dynamics of impact that debris flow has on them.
	Leonardi et al. (2016)	Use of numerical models to represent the interaction between the debris flow and the flexible barrier, in order to design it.
	Huo et al. (2017)	Analysis of the dynamic behaviour of the debris flow in flume tests by varying the volume, concentration and distance travelled before interception by a flexible barrier
	Li and Zhao (2018)	With the help of CFD-DEM, the deformation, storage capacity and failure mechanisms of a flexible barrier due to debris flow were analyzed.
	Jiang et al. (2020)	Use of PFC3D software to evaluate the deformation and failure of the flexible barrier due to the debris flow impact.

In essence, one single equation provided by Rimböck (2004) exists for computing LW-related headlosses, nonetheless, no validation seems to have been performed. No observation of LW overtopping structures exists neither in the lab nor in the field. Recently, the work done by Piton et al. (2020) demonstrated that overtopping do occur on rigid barriers. The following chapters are aimed to analyze both questions.

Chapter 3

Methodology

3.1 Similitude

3.1.1 Fluid mechanics similitude

In free-surface flows, the effects of the gravity force are predominant, therefore the Froude number, Fr, is always significant (Chanson, 2004a). To transfer the experimental results from the model to the real-world prototype we use Froude similitude,

$$Fr_M = Fr_P \tag{3.1}$$

where the subscripts M and P correspond to the model and prototype. From this similarity the following ratios are derived (Heller, 2011):

TABLE 3.1. Scale ratios used in this research.

	Discharge Q (m^3/s)	Force F (N)	Length L (m)	Time t (s)	Velocity u (m/s)	Volume V (m^3)
Scale ratio	$\lambda^{5/2}$	λ^3	λ	$\lambda^{1/2}$	$\lambda^{1/2}$	λ^3

where λ is the scale ratio between the prototype and the model. For this study, it was determined based on approximate dimensions that were originally set for the model and prototype, then, $\lambda = 40$.

3.1.2 Flexible barrier mechanical similitude

One peculiarity of flexible barriers is that they deform under the loads associated to the flow. Here we present concisely how mechanical similitude of the net is approached.

In essence, the flexible barrier is supposed to deform in the elastic domain. Its deformation is driven by: (i) the stiffness of the main cables holding the net and (ii) the stiffness of the net itself. The cables of a flexible barrier are usually made of steel, whose Young modulus ranges from 100-160 GPa. For this investigation, steel will be considered as the construction material for net and cable.

We can assume that both the cables and the net deform only in traction. Then, the relative elongation or strain ε of the cables can be described by a Young modulus E (Pa). :

$$\varepsilon = \frac{F}{E \times A_c} = \frac{F_P}{E_P \times A_{c,P}} = \frac{F_M}{E_M \times A_{c,M}} \tag{3.2}$$

with F the traction force (N), A_c as the area of the cable section (m^2, equal to $\pi\phi_c^2/4$ for round cables with ϕ_c the cable diameter (m)).

This can be rearranged to compute the Young Modulus of the model depending on the prototype Young modulus, forces and sections. Then, applying geometrical scaling and Froude similitude:

$$E_M = E_P \frac{F_M}{F_P} \frac{A_{c,P}}{A_{c,M}} = E_P \frac{1}{\lambda^3} \lambda^2 = \frac{E_P}{\lambda} \tag{3.3}$$

In the case of the net, the strain ε is computed with an equivalent stiffness κ_L (kN/m/m of net) defined by $\Delta l_n = \frac{F/b_n}{\kappa_L}$, with Δl_n the elongation of the sample (m), b_n the width of the sample (m) and F the traction force (N). This approach is similar to the stiffness of a spring, enabling to compute the net deformation:

$$\varepsilon = \frac{\Delta l_n}{l_n} = \frac{F/b_n}{\kappa_L}\frac{1}{l_n} \tag{3.4}$$

with l_n the length of the sample in the traction axis (m).

Thus similarly to the cable, the net equivalent stiffness is scale according to:

$$\kappa_{L,M} = \frac{\kappa_{L,P}}{\lambda} \tag{3.5}$$

This approach was tested on numerical moodels (Abaqus and YADE) and proved relevant (Gonin et al., 2017; Li et al., 2018).

3.2 Experimental set-up

3.2.1 Flume

The experiments were conducted in a 0.40 m wide, rectangular cross-sectional tilting flume, made of glass walls and a wooden bed, supported by an aluminium structure (Figure 3.1). The bed slope set for all the experiments was, $S_0 = 2\%$.

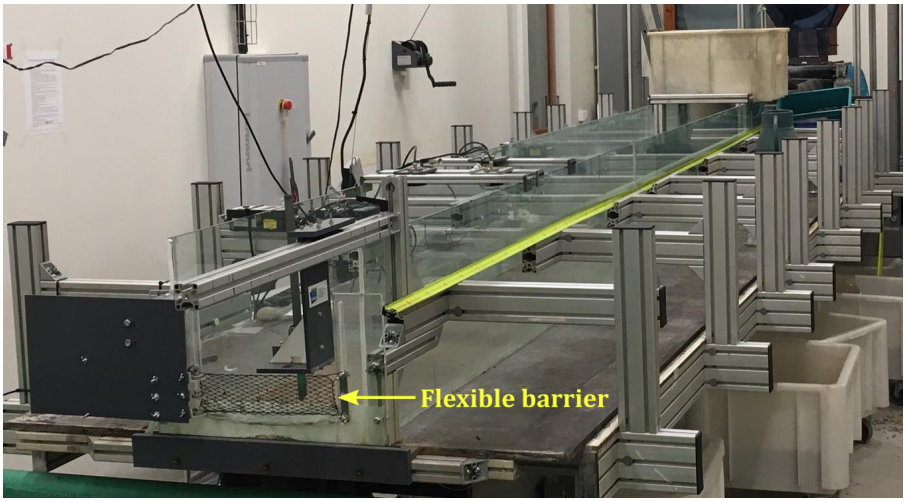

FIGURE 3.1. Experimental scale model.

3.2.2 Flexible Barrier

We worked together with the company Fab&Co to design and choose the material for the net and the cables, which were later manufactured with a 3D printer. The results of a series of tests (traction tests) were presented to determine a material that would satisfy $E_M A_M = E_P/\lambda \cdot A_P/\lambda^2$. For this research, the prototype's cables have a diameter of 24mm and are made of steel, with Young modulus equal to $E_P = 100 - 160$ GPa, which was also used in the prototype's net. With $\lambda = 40$, then, $E_P = 2.5 - 4.0$ GPa; $A_M = 2.87 \cdot 10^{-7}\text{m}^2$ and $E_P/\lambda \cdot A_P/\lambda^2 \approx 706 - 1130$ N.

Since it was not possible to print round cables, the cables were printed in a rectangular shape and with dimensions 0.6×0.9 mm; on plastic PETG (polyethylene terephthalate glycol) with $E \approx 1.3$ GPa. Although this material does not exactly meet the Young modulus established for the model, it was tested to confirm the effectiveness and resistance necessary for this study. Then, the final set for the model $E_P = 1.3$ GPa; $A_M = 5.4 \cdot 10^{-7}\text{m}^2$ and $E_M A_M \approx 702$ N, i.e., is very close from the target value.

The dimensions of the net in the model are 90 × 290 mm. It was printed with a diamond pattern, which simulates the rings of a full-scale net when they are subjected to tensile forces. The plastic TPE (thermoplastic elastomer) was used for the net and has $\kappa_{L,M} \approx 9$ kN/m/m which is close from the downscaled value of the prototype net $\kappa_{L,P}/\lambda \approx 300/40 = 7.5$ kN/m/m. Similar to cables, the equivalent stiffness is slightly below the required value; however, it was decided to use both materials in order to provide more elasticity to the flexible net.

Two vertical and two horizontal cables were used to support the net, with lengths of 0.9 and 0.35m respectively. The net and cables were installed with screws on an Plexiglas support (Fig. 3.2) located at the downstream end of the flume.

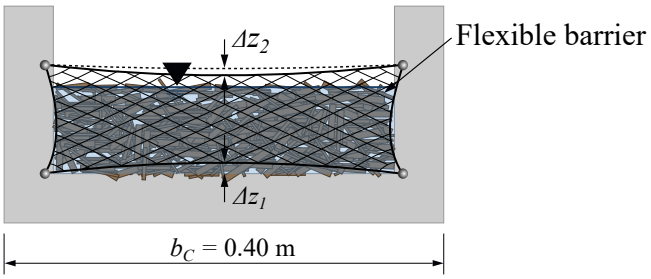

FIGURE 3.2. Front view of the flexible barrier installed at the downstream end of the flume.

3.2.3 LW Mixture

The LW used in the model was a mixture of wood and fine material that in real scale represents large logs and branches, as well as leaves, branches and parts of the roots, respectively.

In the mixture, the wooden part weights 1.3 kg and is composed of floating elements, distributed according its length as follows: 35% elements of 0.05m, 35% elements of 0.1m, 20% elements of 0.15m and 10% elements of 0.20m (table 3.2). The diameters of the components vary between 0.05 m and 0.20 m and were taken from the Serb tree (*Sorbus Aucuparia*), common in the lowlands.

TABLE 3.2. Distribution of the wooden elements in the model.

Length of logs, L_{LW} (m)				Mean Length	Mean Diameter	Solid Volume	Wood Density
0.05	0.10	0.15	0.20	$L_{LW,mean}$ (m)	$\phi_{LW,mean}$ (m)	V_s $(10^{-3}, m^3)$	ρ_w (kg/m^3)
330	130	60	20	0.08	0.075	2.04	770

Pine needles were used as fine material, FM. According to Schalko (2018), it is recommended that the fine material content should be 3-15% of the weight of the wood, however, for this research 20% was consequently used, i.e. 0.26kg of pine needles were added, see table 3.3.

TABLE 3.3. LW features for the model.

	Weight W_{LW} (Kg)	Volume V_s (m^3)
Wood	1.3	$1.3 \cdot 10^{-3}$
Fine material, FM	0.26	$2.3 \cdot 10^{-3}$

At the beginning of the tests, the wood was dry (not green wood). On the contrary, the pine neddles were collected a few days before the beginning of the experiments, so they were "fresh" when the experiments started. Once the experiments began, the density, mass, and volume of the wood changed due to the water content, which was maintened at each experiment by weighting the whole mixture.

3.3 Instrumentation

3.3.1 Parameters to be measured

The following parameters were considered key drivers or responses of the system and were measured:

- Discharge, Q (m^3/s)
- Length of LW carpet, L_A (m)
- Vertical deformation of the top of the flexible barrier, Δz_2 (m)
- Water depth without LW, h_0 (m), and with LW, h (m)
- Weight of elements leaking from the barrier due to bottom clearance, $W_{LW,Out}$ (Kg)
- Weight of the LW mixture input in each experiment, $W_{LW,In}$ (Kg)

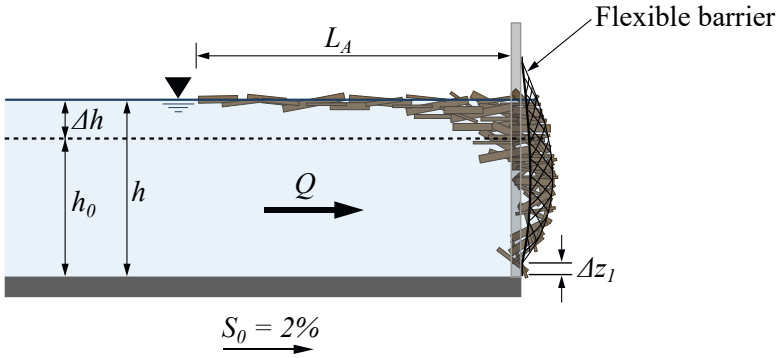

FIGURE 3.3. Schematic profile view of the experimental set-up and identification of the parameters.

3.3.2 Discharge

The flow inside the channel is in a closed circuit composed of two pumps mounted in parallel. The maximum discharge capacity is ≈ 8 l/s and is measured with an electromagnetic flow-meter. A tank with a capacity of 2200 liters is used to recover the water and filter it for later re-circulation within the circuit.

3.3.3 Water depth

An instrument built at INRAE and composed of a digital Vernier scale, was installed at the top of the channel, just above the flexible barrier. This device was used to measure the water depth as well as the vertical deformation of the net Δz_2 (figure 3.2).

3.3.4 LW sample weight

With a digital scale, we measured the weight of the material that was released through the barrier and/or overtopped it.

3.3.5 Record Form

The beginning, end and steps of each test were recorded in a format where the discharge was also noted for each step. In the same sheet, the height of the water (h, h_0), the length of the LW carpet (L_A), the net crest (z_2), the weight of the introduced mixture ($W_{LW,In}$) and the weight of the material that was released ($W_{LW,Out}$), were written in each step.

3.4 Experiment series

For each experiment the water depth was measured with and without LW to determine the head losses, the flow pattern of the logs was examined and the discharge that causes overflowing and LW overtopping was found.

Each run started with a discharge of 1 l/s and ended until reaching 8 l/s (approximately) or overtopping, whichever occurred first. The water discharge increased step by step, with a progressive increase ranging from 0.5 to 1.5 l/s. The water level and the upper vertical deformation of the network were measured once the discharge was stable, i.e. approximately 3 minutes after the transitional period related to the change from one discharge stage to another. During each step, the released LW were weighed and the length of the carpet created by the LW was measured.

Two conditions were considered her for the experiments: unobstructed and obstructed barriers. The unobstructed is the condition where the net is at its maximum efficiency, no log is trapped in it. The obstructed is a condition where the net is partially clogged by trapped logs. For the second condition, a plastic sheet was placed on the net to simulate the clogging (see Fig. 3.4). In order to analyze the different obstruction conditions, 3 series of experiments were performed. Therefore, a total of 4 series of experiments were performed as follows:

- Series 1. Net free, without any kind of obstruction.
- Series 2. Net with a 5 cm high plastic sheet.
- Series 3. Net with a 5 cm high perforated plastic sheet.
- Series 4. Net with a 3 cm high plastic sheet.

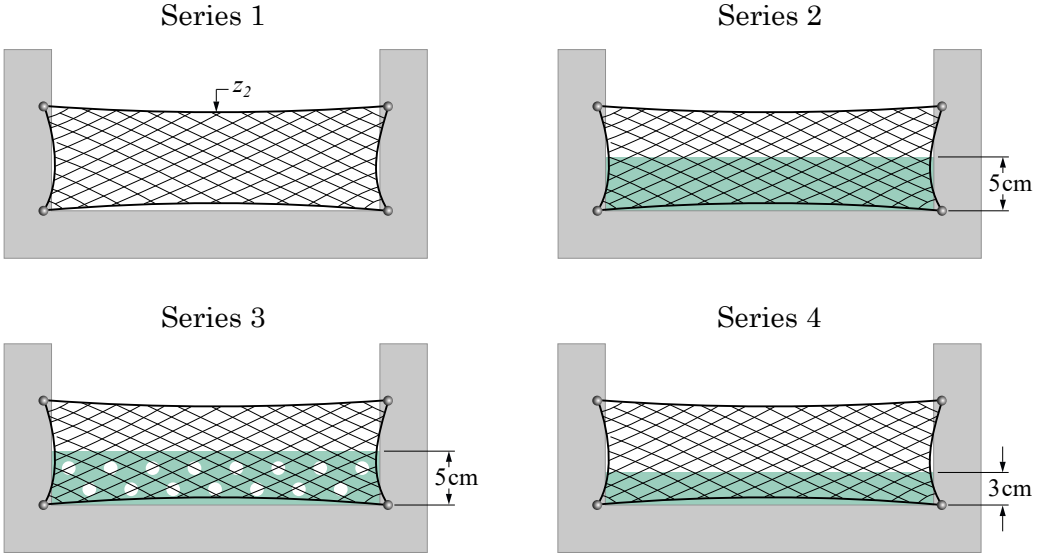

FIGURE 3.4. Division of experiments into series.

As mentioned in section 1.2.3 and according to figure 1.4a, the regime **congested** was defined for this investigation. To fulfill this condition and knowing that the carrying and travel of the LW in a river is random and difficult to predict, the mixture was manually introduced into the channel approximately 2 meters upstream of the net, in 4 different ways:

- Whole mix: It was put from the first step and spread along the channel, in order to avoid possible accumulations before reaching the net.
- 1/3 of the total weight of the mixture: Before starting each run for this condition, the mixture was weighted and split into 3 portions of approximately the same weight. The first part was spread on the flume in the first step, the second part during the second discharge step and the third part at the beginning of the third discharge step.

- 1/6 of the total weight of the mixture: The mixture was weighted and then split into 6 portions that weighted approximately the same. The first part was spread on the flume in the first step, the second part during the second step, the third part at the beginning of the third step and so on until the sixth step was reached.
- 1/7 of the total weight of the mixture: The same methodology was followed as with 1/3 and 1/6, only this time the mixture was split into 7 portions and spread on the channel progressively until reaching the seventh step.

For each series, three runs were made with the conditions detailed before and a clear water run (no wood), in order to calibrate the model and establish water levels without wood, see figure 3.5. In addition, in series 3 and 4, a piece of fabric was introduce at the end of the experiment below the floating carpet. It flowed to the logs accumulated against the net, reduced even more the permeability of the system and increased water depth until overtopping occured. This was an experimental adaptation to actually observe the overtopping process.

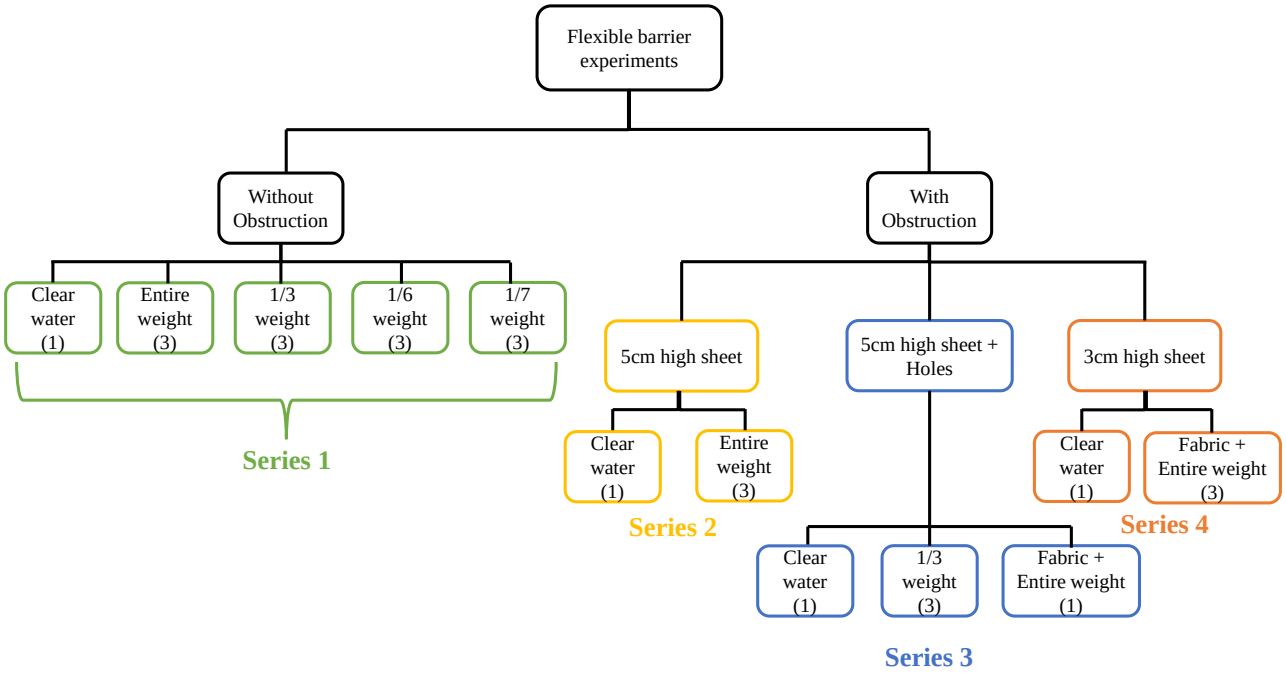

FIGURE 3.5. Different series of experiments carried out

In Appendix B, some pictures of the experiments carried out are shown, while in Appendix C a table with the measurements made for every step of each series is attached.

Chapter 4

Results

For the purpose of easier interpretation, the results of the experiments performed are presented as follows: (i) qualitative description of the interaction between the LW and the flexible barrier, (ii) estimation of head losses and comparison with equations from other authors and (iii) release condition.

4.1 LW flow behavior

Within this research, the LW flow was divided into 3 phases, in order to be characterized (Figure 4.1):

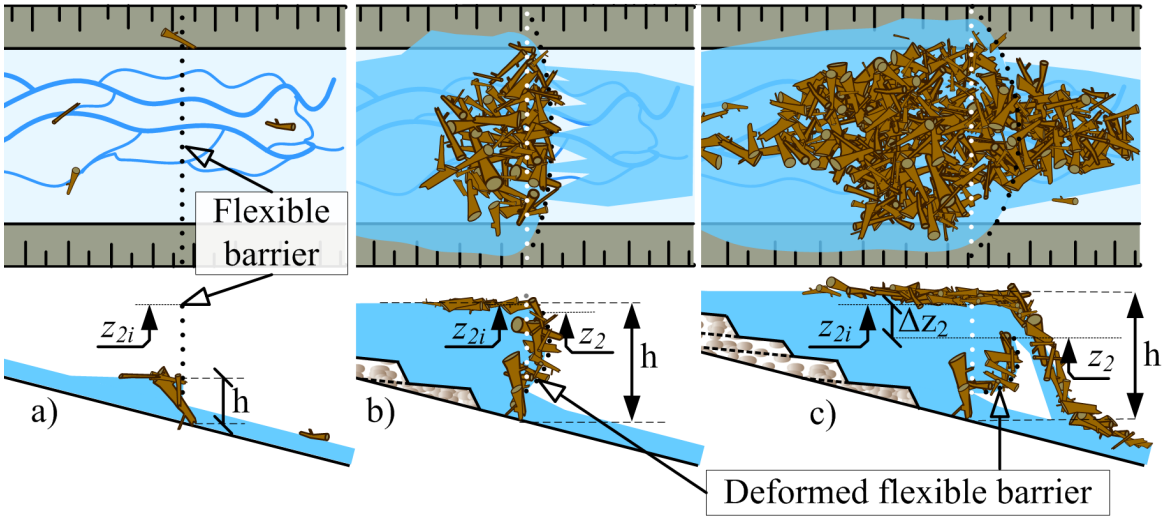

FIGURE 4.1. Main phases of LW trapping in a flexible barrier: a) initial trapping phase against the barrier, b) overflowing atop the barrier crest while entangled logs remains in the barrier, and c) final overtopping of the floating carpet

- **Phase 1: Accumulation against the dam (Figure 4.1a).**

  Once the water flow started and with the LW inside the flume, the elements started to run through the flume until they reached the flexible barrier, where some elements of the LW passed through the bottom clearance, especially in Series 1 and with the runs of 1/6 and 1/7 of the total weight. This was due to the absence of any obstruction as well as the few material that was put in and was not able to be retained in order to create a log barrier. Those elements that were retained by the dam, became stuck in it and often parallel to it.

  As the discharge in the steps was increased, the water level also rise until it reached a stable value. The LW settled in the dam causing a blockage by accumulation of the cross section of the dam, taking a triangular shape (Figure 2.2).

  The elements that formed the new block of logs were: (i) floating freely and moving with the flow, (ii) forming a LW carpet that increased in length in each of the steps, except in the cases

in which the total volume of the mixture was put in the first step, because due to the push of the water, the compaction of the carpet was caused, or (iii) dragged under the carpet and driven to the flexible dam, this behavior was observed mainly with the pine needles.

- **Phase 2: Overflowing with possible LW release (Figure 4.1b).**

  It is considered phase 2, once the overflowing is reached, that is, when the water level (with or if LW) exceeds the height of the flexible barrier. This was usually observed in the last steps of the process, and in the series where there was an obstruction. The LW carpet was jamming at the level of the free surface and above the crest of the dam, and even though it appeared that the the basin was submerged, only a few wands helps to entangled logs about the net, preventing then the overtopping (Piton et al., 2020).

  The LW flow stuck on the net in addition to the LW carpet and the water flow caused a total pushing on the net, which was totally arched and allowing only water to pass through the porosity of the blockage created by the accumulation of elements in the cross section of the dam.

- **Phase 3: Actual LW release (Figure 4.1c).** Due to the limitation of the pumping system, it was not possible to obtain this phase in all the series and it was only obtained in the series with an obstruction (Series 2, 3, 4). Furthermore, to achieve a total release of LW it was necessary to add a piece of fabric, submerge it and introduce it upstream to make another blockage in the cross section of the dam, thereby increasing the water level and having the desired effect. On two occasions, the upper horizontal cable broke due to the force applied by the LW flow, so it had to be replaced.

4.2 Head losses

In order to meet one of the main objectives of this research, the calculation of head losses were studied, i.e., the increase of water level as a consequence of the LW flow in a channel. The results obtained in the experiments were plotted and compared with equations proposed by several authors.

4.2.1 Effect of discharge and mass of LW on water depth

Figure 4.2 shows the results of the Series 1 experiments, where the water elevations against discharge are plotted. As we expected, h increases with Q.

To obtain a better approximation of the flow behaviour the equation 2.8 was used. In the investigation carried out by Piton et al. (2020), the coefficient μ was calibrated, resulting in a value equal to 0.65 for thin-dam-configuration, which is applicable in the flexible barrier.

Likewise, in the research made by Piton et al. (2020) to calculate the head losses in different rigid barriers, they use $\beta_{min} = 0.5$ and $\beta_{max} = 1.1$ for a SABO dam. It was tested to use the same value of both coefficients in the flexible barrier.

The application of the β factors provides similar approximation of the lower and upper limits, respectively, of almost all the 10 experiments performed for Series 1. The graph describes that overflowing was rarely achieved and never overtopping. When the full weight of the sample was added from the start of the test, overflowing or overtopping is less likely to occur.

Also, the relationship of the water level rise to the volume of LW added to the channel was graphed. This is shown in Figure 4.3 and corresponds only to the series 1 experiments.

Even though the results are more widely dispersed than in the previous graph and there is no trend line as such, in the graph it can be seen that the increase in water level is correlated to the amount of LW introduced into the channel, no matter if the total weight was put from the beginning or if it was done in portions at each step.

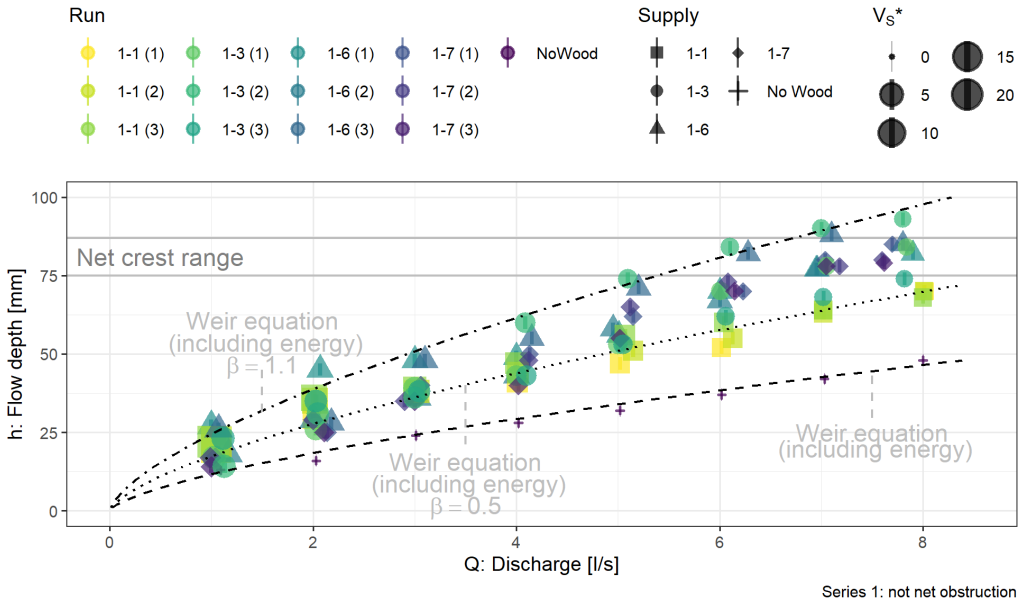

FIGURE 4.2. LW-related head losses and stage-discharge relationships for Series 1.

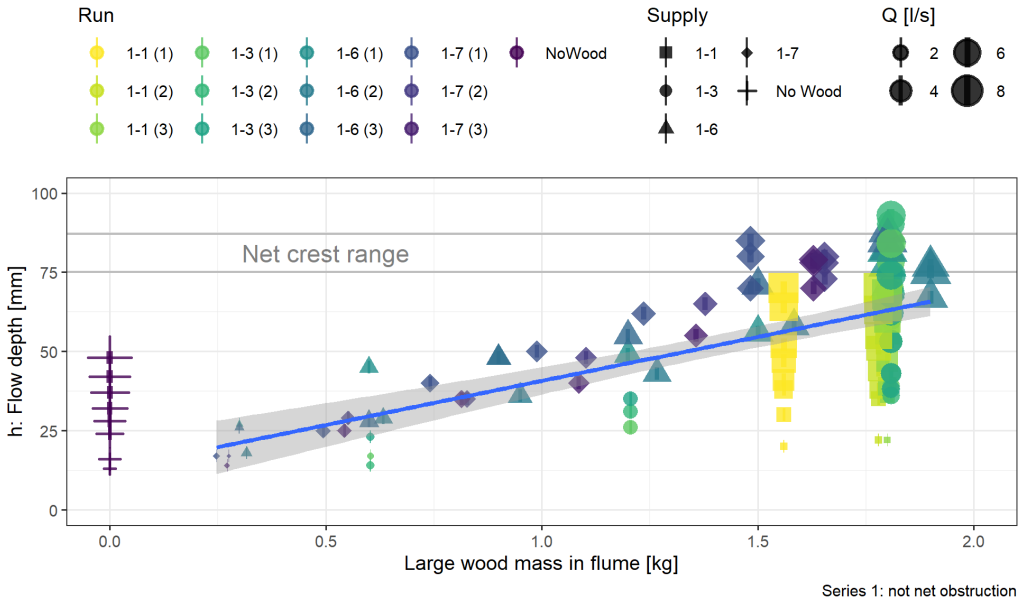

FIGURE 4.3. Flow depth versus large wood mas in flume for flexible barrier.

4.2.2 Development of a new approach for Head Losses

Schalko et al. (2019a) used the following way to make the large wood volume dimensionless defining the relative LW solid volume:

$$V_s^* = \frac{V_s}{3.1 Fr_0 b_C h_0^2} \tag{4.1}$$

They demonstrate that headloss increases very rapidly until $V_s^* = 1$ and then the floating carpet forms and the headloss increase more slowly with increasing LW volume. In essence, $3.1 Fr_0 b_C h_0^2$ is a critical volume sufficient to jam the barrier.

Meanwhile, Piton et al. (2020) introduced a new dimensionless number called buoyancy to drag force ratio, $\frac{\Pi}{F_d}$, interesting for the analysis of LW dynamics and it is computed as the ratio between

buoyancy (Π) and drag force (F_d) whose first approximation can be:

$$\frac{\Pi}{F_d} = \frac{g(\rho - \rho_s)\pi\phi_{LW,mean}^2 L_{LW,mean}/4}{C_D\rho\phi_{LW,mean}L_{LW,mean}u^2/2} = \frac{\pi}{2C_D}\frac{\rho - \rho_s}{\rho}\frac{\phi_{LW,mean}}{h}\frac{gb_C^2h^3}{Q^2} \tag{4.2}$$

where C_d is the drag coefficient and is taken equal to 1.2 for logs without branches, ρ and ρ_w is the water and LW density, respectively (kg/m^3), b_C is the width of the channel (m), Q the flow discharge (m^3/s), $\phi_{LW,mean}$ the mean log diameter of the LW mixture (m), $L_{LW,mean}$ the mean log lenght (m), u is the flow velocity close to the log which is approximated here by $u = Q/hb_C$.

Figure 4.4 compare Π/F_d vs V_s^* for the data obtained from the Series 1 experiments. For the case where the total volume was added from the beginning of the experiment, it is observed that there is a consistent increase in $\frac{\Pi}{F_d}$ with an increase of the relative LW solid volume. $\frac{\Pi}{F_d}$ being proportional to the h^2, it means that depth increases with large wood amount which is intuitive and consistent with theory (Rimböck, 2004; Schmocker and Hager, 2013; Schalko et al., 2019a).

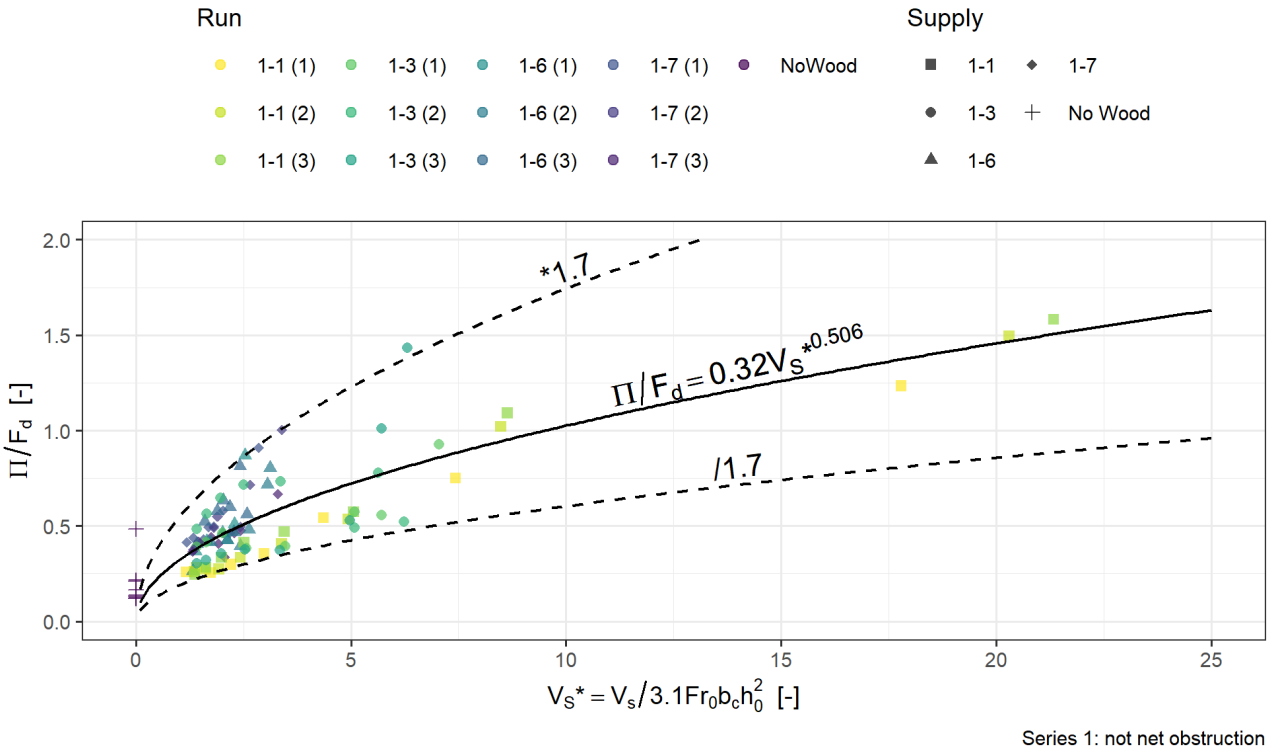

FIGURE 4.4. Pi/Fd VS V_s^*.

Then, from figure 4.4 the best fit gives:

$$\frac{\Pi}{F_d} = 0.32 \times V_s^{*0.506} \tag{4.3}$$

It is possible to compute h if the equation 4.3 is rearranged in :

$$h = \sqrt{\frac{0.32 \times 2C_D}{\pi g\phi_{LW,mean}}\frac{\rho}{(\rho - \rho_s)}\frac{Q}{b_C}}\left(\frac{V_s}{3.1Fr_0b_Ch_0^2}\right)^{0.253} \tag{4.4}$$

The use of the equation 4.4 is compared against the measured data for Series 1 and proves satisfying (Figure 4.5a). In addition it is based on dimensionless numbers and is thus more likely to be relevant when up-scaled. The linearity of the increases of depth with discharge and with the volume of wood to a power between 0.2 and 0.33 are both quite consistent with previous results of Rimböck (2004); Schmocker and Hager (2013); Schalko et al. (2019a).

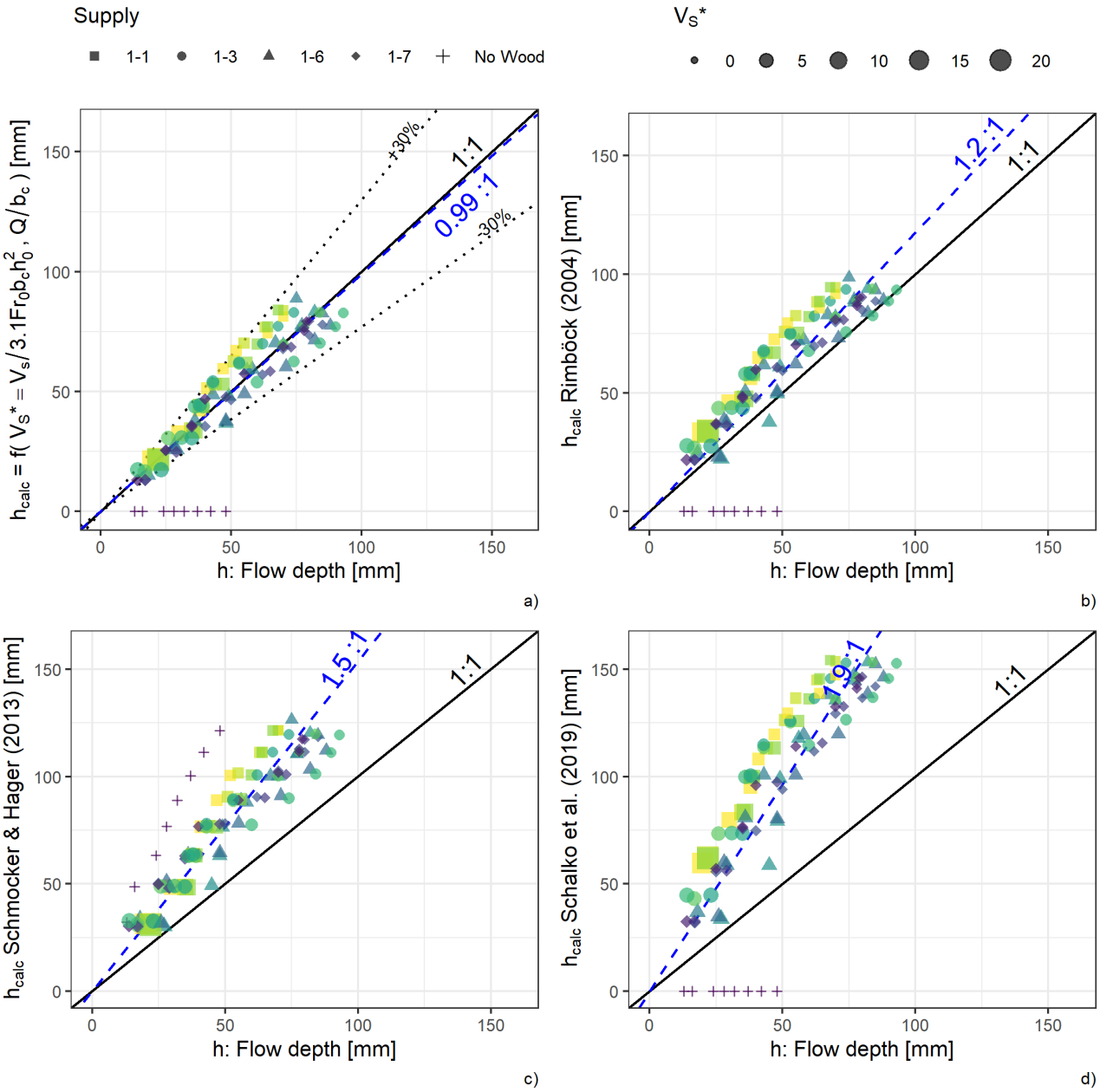

FIGURE 4.5. Computed depth compared to measured depth (Series 1 only): a) new approach of Eq. (4.4), b) Rimböck (2004) approach of Eq. (2.11), c) Schmocker and Hager (2013) approach of Eq. (2.2), and d) Schalko et al. (2019a) approach of Eq. (2.5)

4.2.3 Applicability of existing equations

Rimböck (2004)'s Equation

By applying the default values for the model to equation 2.11, it is possible to compute h. The results obtained by applying the equation and the measured data from the Series 1 experiments were compared and are shown in Figure 4.5b.

Although the Rimböck equation takes into account parameters such as the percentage of fine material (FM) as well as the solid volume (V_s) in the experiment, it is possible to observe that the results of the head losses are overestimated with respect to equation 4.4, although they are close to it. While the results are fairly close in the flume experiment, equation 2.11, not being based on dimensionless numbers, shows deviation when upscaled as demonstrated in the Appendice A: according to the computation, the maximum pump discharge (upscaled at prototype scale) should reach a depth of 7.7/40=193mm while we observed a maximum depth of about 100 mm in the flume.

Schmocker and Hager (2013)'s Equation

With the equation that Schmocker proposed (2.2), it was also possible to estimate h. This is the simplest equation presented in this research related to the estimation of head losses. The results are shown in Figure 4.5c, and as in the case of Rimböck, the head loss is overestimated with respect to the new approach. It is important to mention that the Schmocker equation for the calculation of head losses, only takes into account the Froude number, so it is always recommended to compare it with a method that considers the LW flow.

Schalko et al. (2019a)'s Equation

Finally, head losses were computed with the equation proposed by Schalko, equation 2.5. The results are shown in Figure 4.5d, where, as in the previous cases, it can be seen that the head losses are even more significant than those calculated by the new approach. This is probably due to all the parameters that Schalko considered for the calculation, such as the accumulation of the elements (f_a), the diameter of the elements, etc. Although this seems to be the most conservative method to obtain head losses, it is not recommended if you do not want to obtain an overdesigned net.

4.3 Release conditions

The second objective of this research is the analysis of the release condition. As explained previously, it was necessary to generate a blockage with an obstruction of the net, in this case a plastic sheet placed at different elevations of the flexible barrier and in some cases to introduce an additional piece of fabric (in Series 3 and 4), in order to decrease the porosity of it and then, cause the water depth to increase sufficiently to generate massive released over the structure. Indeed, no overtopping was observed during Series 1 of experiments. That is why Series 2-4 were launched with varied obstruction of the net (recall Figure 3.4 and 3.5).

The measured depths and net crest levels with varying discharge are displayed in Figure 4.6 with dot size proportionnal to the released amount of LW (normalized by the total volume of the mixture). Obstructed barrier generated obviously higher depth for similar discharges. Net crest levels (light grey lines) decrease with increasing discharge and water depth because of the barrier deformation. Although overflowing does occur in Series 1 for some experiments on discharge higher than 6 l/s, no releases were observed (small dot size). Conversely, large releases were observed on Series 2-4 for sufficiently high overflowing. Obstructed barriers tend also to deform more (gray lines being lower).

All these experiments can be studied in a dimensionless way using equation 2.9, the dimensionless overtopping depth $h^* = \frac{h-z_2}{\phi_{LW,m}}$. This function of the average diameter of the logs, the height of the crest as well as the water depth with LW, was used by Piton et al. (2020) to study releases over rigid barriers. They observed that most releases occur for h^* in a range 3-5 but a couple of particularly dense accumulations with entangled logs were released for h^* approaching 10. All these parameters were measured in each of the experiments, so it was possible to calculate h^* and subsequently plot it against the percentage of LW released for a given discharge step (Figure 4.7).

It is observed that, although the flexible barrier is quite different from rigid barriers, the releases seem to occur above a similar threshold value h^* than in rigid barriers, i.e., above 3 and up to 10. The number of large releases being fairly small, we cannot conclude on the applicability of the approach immediately. In addition, we suspect that the obstruction of the net might modify the way LW piled up and thus the overall stability of the accumulation. New series of experiments with lower nets will be launched to check the relevance of the approach. The effect of LW mixture features (mean diameter, lenghts) will also be addressed.

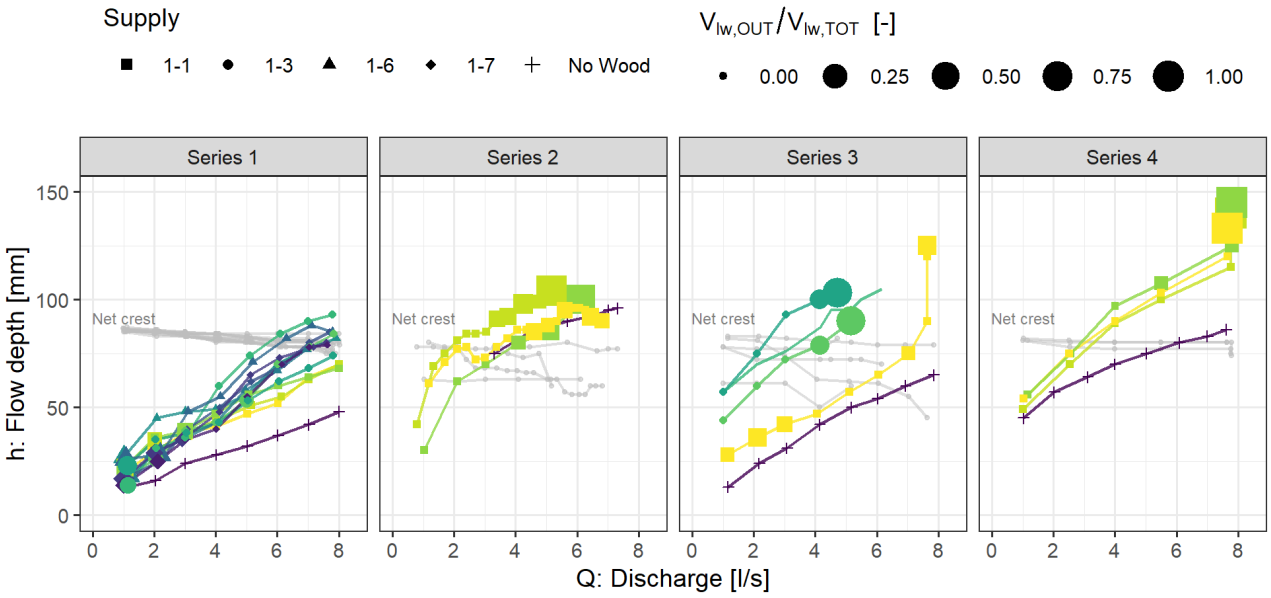

FIGURE 4.6. Depth against discharge for all series. Grey lines represent the crest of the net. Each run has a different color.

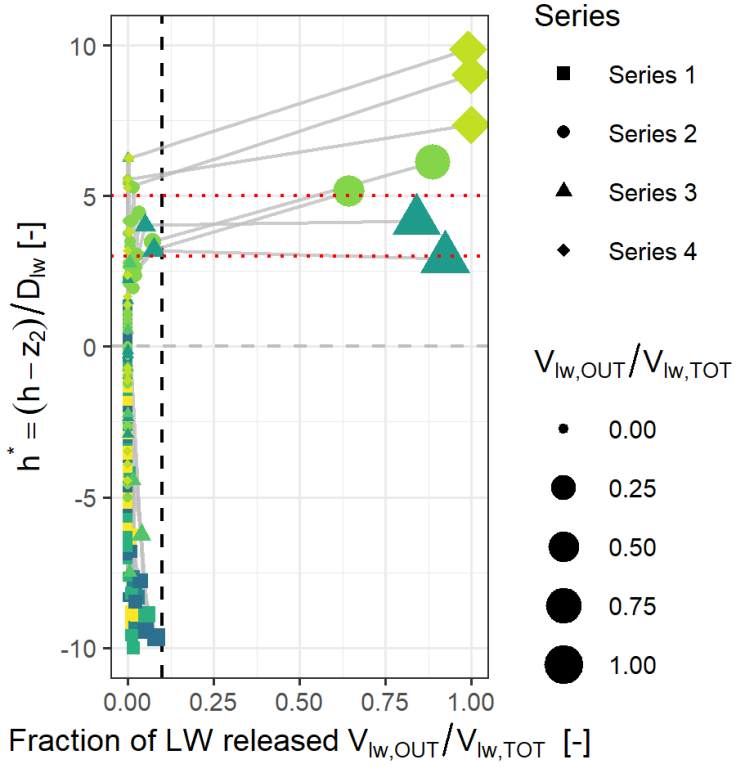

FIGURE 4.7. Release condition.

Chapter 5

Conclusions

The main function of an open check installed on a river, is the trapping of solid material (sediment or large wood) to mitigate and control possible damages that certain events can cause in the neighbourhood because solid transport worsen flow conditions. Such events include debris flow and LW flow, which are difficult to predict and therefore difficult to control. For several years now, numerous investigations have been carried out in order to characterise these flows and the barriers capable of controlling them. Rigid and flexible barriers have been tested on scale models within laboratories and subsequently on real structures. The effectiveness of the barriers is conditioned by certain parameters such as their design and geometry, which depend on the site of installation and the conditions to which they will be subjected.

Nowadays, the literature concerning LW flow has been growing and there are many articles and even books, whose main topic is wood in rivers. Thanks to this, it has been possible to deepen and propose new forms of control, as well as possible benefits for nature. However, certain issues have been ignored or not given enough attention, thus missing out on potential areas of opportunity.

In an effort to find practical alternatives, this research was aimed at studying the effects of LW on a flexible barrier, with emphasis on head losses and release conditions. A new approach was developed for the calculation of head losses, in which we tried to include as many parameters as possible related to LW flow. In combination with the new approach, a series of experiments were conducted where the discharge was varied, as well as the amount of wood introduced into the channel. By comparing the results with the new approach and with equations developed by other authors, it was found that the increase in water level is related to the discharge (as expected) and the LW flow features (volume, density and diameter).

Concerning the release condition, flexible barriers were shown to have good effectiveness as a method of containing LW flow. In fact, it was necessary to generate a blockage in order to find an overtopping condition. In essence it was observed that overtopping appear when water level above the net crest is typically about 2-5 times the LW mean diameter. With respect to the amount of material released through the bottom clearance, it is important to mention that this value is fundamental when designing a flexible barrier. A wide opening favours the loss of entrapment, while a small opening blocks the barrier quickly, diminishing its capacity. Also, the fine material plays an important role in the trapping. The leaves and branches, promote the conditions of entanglement of logs in the flexible barrier, creating then a longitudinal carpet of LW and reducing the possible overtopping. It is expected to continue with more experiments and with more conditions that will help to demonstrate and deepen several of the points covered in this research.

List of Symbols

Δh	Head loss, m.
Δl_n	Elongation of the sample, m.
κ_L	Equivalent stiffness of the net, kN/m/m.
λ	Geometrical scale ratio between model and prototype.
μ	Weir coefficient.
ϕ_c	Diameter of the cable, m.
$\phi_{LW,m}$	Mean diameter of the logs in the model, m.
Π/F_d	Bouyancy to drag force ratio.
ρ	Water density, kg/m^3.
ρ_w	Wood density, kg/m^3.
ε	Elongation, m.
a	Bulk factor corresponding to the compactness of LW volume.
A_c	Cable cross-sectional area, m^2.
b_B	Flexible barrier width, m.
b_C	Channel width, m.
b_n	Width of the sample, m.
b_W	Weir width, m.
c	Coefficient based on channel slope S_0, Rimböck equation
E	Young modulus, Pa.
F	Traction force, N.
f_A	Accumulation type factor.
FM	Fine material, %.
Fr_0	Froude number of the flow without LW.
h	Water depth with LW, m.
h^*	Dimensionless overflowing depth = $(h - z_2)/\phi_{LW,m}$.
h_0	Initial water, m.
h_{DF}	Water depth of Debris Flow, m.
K	Strickler coefficient, m$^{\frac{1}{3}}$/s.
L_A	Length of wood carpet, m.
l_n	Length of the cable in the traction axis, m.
$L_{LW,m}$	Mean length of the logs in the scale model, m.

L_{LW} Length of the logs in the scale model, m.

Q Discharge, m3/s.

q Unit discharge, m2/s.

$Q_{LW,in}$ Large wood input rate, m3/s.

S_0 Slope of the channel bed.

u Flow velocity, m/s.

V_s^* Relative LW solid volume.

V_s Solid volume of LW, m^3.

V_{LW} Volume of LW incluiding voids, m^3.

$W_{LW,In}$ Weight of the input LW mixture in the model, kg.

$W_{LW,Out}$ Weight of the output LW mixture in the model, kg.

W_{LW} Total Weight of LW mixture, kg.

z_1 Bottom clearance, m.

z_2 Crest level, m.

Bibliography

Addy, S. and Wilkinson, M. E. (2019). Representing natural and artificial in-channel large wood in numerical hydraulic and hydrological models. *Wiley Interdisciplinary Reviews: Water*, 6(6):e1389.

Anderson, N. H., Sedell, J. R., Roberts, L. M., and Triska, F. J. (1978). The Role of Aquatic Invertebrates in Processing of Wood Debris in Coniferous Forest Streams. *American Midland Naturalist*, 100(1):64.

Andrus, C. W., Long, B. A., and Froehlich, H. A. (1988). Woody Debris and Its Contribution to Pool Formation in a Coastal Stream 50 Years after Logging. *Canadian Journal of Fisheries and Aquatic Sciences*, 45(12):2080–2086.

Armanini, A., Dellagiacoma, F., and Ferrari, L. (1991). From the check dam to the development of functional check dams. In Armanini, A., Di Silvio, G., Bhattacharji, S., Friedman, G. M., Neugebauer, H. J., and Seilacher, A., editors, *Fluvial Hydraulics of Mountain Regions*, volume 37, pages 331–344. Springer Berlin Heidelberg, Berlin, Heidelberg.

Bichler, A., Yonin, D., and Stelzer, G. (2012). Flexible debris flow mitigation: introducing the 5.5 mile debris fence. *Landslides and engineered slopes: protecting society through improved understanding. CRC Press, New York*, pages 1955–1960.

Bocchiola, D., Rulli, M. C., and Rosso, R. (2008). A flume experiment on the formation of wood jams in rivers: EXPERIMENT ON WOOD JAMS. *Water Resources Research*, 44(2).

Braccia, A. and Batzer, D. P. (2008). Breakdown and invertebrate colonization of dead wood in wetland, upland, and river habitats. *Canadian Journal of Forest Research*, 38(10):2697–2704.

Braudrick, C. A. and Grant, G. E. (2000). When do logs move in rivers? *Water resources research*, 36(2):571–583.

Braudrick, C. A., Grant, G. E., Ishikawa, Y., and Ikeda, H. (1997). Dynamics of wood transport in streams: a flume experiment. *Earth Surface Processes and Landforms: The Journal of the British Geomorphological Group*, 22(7):669–683.

Brighenti, R., Segalini, A., and Ferrero, A. M. (2013). Debris flow hazard mitigation: A simplified analytical model for the design of flexible barriers. *Computers and Geotechnics*, 54:1–15.

Brooks, A. P., Howell, T., Abbe, T. B., and Arthington, A. H. (2006). Confronting hysteresis: Wood based river rehabilitation in highly altered riverine landscapes of south-eastern Australia. *Geomorphology*, 79(3):395–422.

Brummer, C. J., Abbe, T. B., Sampson, J. R., and Montgomery, D. R. (2006). Influence of vertical channel change associated with wood accumulations on delineating channel migration zones, Washington, USA. *Geomorphology*, 80(3):295–309.

Canelli, L., Ferrero, A. M., Migliazza, M., and Segalini, A. (2012). Debris flow risk mitigation by the means of rigid and flexible barriers – experimental tests and impact analysis. *Natural Hazards and Earth System Sciences*, 12(5):1693–1699.

Chanson, H. (2004a). *Hydraulics of open channel flow*. Elsevier.

Chanson, H. (2004b). Sabo check dams - mountain protection systems in Japan. *International Journal of River Basin Management*, 2(4):301–307.

Comiti, F., Lucía, A., and Rickenmann, D. (2016). Large wood recruitment and transport during large floods: a review. *Geomorphology*, 269:23–39.

De Cicco, P. N., Paris, E., Ruiz-Villanueva, V., Solari, L., and Stoffel, M. (2018). In-channel wood-related hazards at bridges: A review. *River Research and Applications*, 34(7):617–628.

DeNatale, J. S., Iverson, R. M., Major, J. J., LaHusen, R. G., Fiegel, G., and Duffy, J. D. (1999). *Experimental testing of flexible barriers for containment of debris flows*. US Department of the Interior, US Geological Survey Reston.

Dixon, S. J., Sear, D. A., Odoni, N. A., Sykes, T., and Lane, S. N. (2016). The effects of river restoration on catchment scale flood risk and flood hydrology. *Earth Surface Processes and Landforms*, 41(7):997–1008.

Furlan, P. (2019). Blocking probability of large wood and resulting head increase at ogee crest spillways. Technical report, EPFL.

Gerhard, M. and Reich, M. (2000). Restoration of Streams with Large Wood: Effects of Accumulated and Built-in Wood on Channel Morphology, Habitat Diversity and Aquatic Fauna. *International Review of Hydrobiology*, 85(1):123–137.

Gonin, M., El Moueddeb, M., Fertane, L., Archambaud, J., Godet, N., Colombani, P., Sande Y Mallo, R., Piton, G. G., and Bourrier, F. (2017). Small scale net project: technical report. Technical report, Grenoble INP ENSE3 - IRSTEA. working paper.

Grabowski, R. C., Gurnell, A. M., Burgess-Gamble, L., England, J., Holland, D., Klaar, M. J., Morrissey, I., Uttley, C., and Wharton, G. (2019). The current state of the use of large wood in river restoration and management. *Water and Environment Journal*, page wej.12465.

Gurnell, A. M., Piegay, H., Swanson, F. J., and Gregory, S. V. (2002). Large wood and fluvial processes. *Freshwater Biology*, 47(4):601–619.

Gurnell, A. M. and Sweet, R. (1998). The distribution of large woody debris accumulations and pools in relation to woodland stream management in a small, low-gradient stream. *Earth Surface Processes and Landforms*, 23(12):1101–1121.

Harmon, M. E. and Hua, C. (1991). Coarse Woody Debris Dynamics in Two Old-Growth Ecosystems. *BioScience*, 41(9):604–610.

Hashimoto, H., Hashimura, K., Nagano, H., and Maricar, F. (2016). Experimental Investigation into Flow Behavior of Wood-Sediment-Water Mixture at a Grid Type of Open Check Dam. *International Journal of Erosion Control Engineering*, 9(4):6.

Heller, V. (2011). Scale effects in physical hydraulic engineering models. *Journal Of Hydraulic Research*, 49(3):293–306.

Helmers, A. E. (1966). Some effects of log jams and flooding in a salmon spawning stream.

Hering, D., Kail, J., Eckert, S., Gerhard, M., Meyer, E. I., Mutz, M., Reich, M., and Weiss, I. (2000). Coarse Woody Debris Quantity and Distribution in Central European Streams. *International Review of Hydrobiology*, 85(1):5–23.

Horiguchi, T., Shibuya, H., Katsuki, S., Ishikawa, N., and Mizuyama, T. (2015). A basic study on protective steel structures against woody debris hazards. *International Journal of Protective Structures*, 6(2):191–215.

Huo, M., Zhou, J.-w., Yang, X.-g., and Zhou, H.-w. (2017). Effects of a flexible net barrier on the dynamic behaviours and interception of debris flows in mountainous areas. *Journal of Mountain Science*, 14(10):1903–1918.

James, G. A. (1956). *The physical effect of logging on salmon streams of southeast Alaska*. Alaska Forest Research Center.

Jiang, R., Fei, W.-p., Zhou, H.-w., Huo, M., Zhou, J.-w., Wang, J.-m., and Wu, J.-j. (2020). Experimental and numerical study on the load and deformation mechanism of a flexible net barrier under debris flow impact. *Bulletin of Engineering Geology and the Environment*, pages 1–21.

Keller, E. A. and Swanson, F. J. (1979). Effects of large organic material on channel form and fluvial processes. *Earth Surface Processes*, 4(4):361–380.

Lautz, L. K., Siegel, D. I., and Bauer, R. L. (2006). Impact of debris dams on hyporheic interaction along a semi-arid stream. *Hydrological Processes*, 20(1):183–196.

Leonardi, A., Wittel, F. K., Mendoza, M., Vetter, R., and Herrmann, H. J. (2016). Particle-Fluid-Structure Interaction for Debris Flow Impact on Flexible Barriers: Debris flow impact on flexible barriers. *Computer-Aided Civil and Infrastructure Engineering*, 31(5):323–333.

Li, S., Piton, G., and Bourrier, F. (2018). Scale Effect: Numerical Modeling of Net Barriers in Torrents. Technical report, Grenoble INP ENSE3 - IRSTEA. working paper.

Li, X. and Zhao, J. (2018). A unified cfd-dem approach for modeling of debris flow impacts on flexible barriers. *International Journal for Numerical and Analytical Methods in Geomechanics*, 42(14):1643–1670.

Lienkaemper, G. W. and Swanson, F. J. (1987). Dynamics of large woody debris in streams in old-growth Douglas-fir forests. *Canadian Journal of Forest Research*, 17(2):150–156.

Montgomery, D. R., Buffington, J. M., Smith, R. D., Schmidt, K. M., and Pess, G. (1995). Pool Spacing in Forest Channels. *Water Resources Research*, 31(4):1097–1105.

Nagayama, S., Kawaguchi, Y., Nakano, D., and Nakamura, F. (2008). Methods for and fish responses to channel remeandering and large wood structure placement in the Shibetsu River Restoration Project in northern Japan. *Landscape and Ecological Engineering*, 4(1):69–74.

Nagayama, S., Nakamura, F., Kawaguchi, Y., and Nakano, D. (2012). Effects of configuration of in-stream wood on autumn and winter habitat use by fish in a large remeandering reach. *Hydrobiologia*, 680(1):159–170.

Piegay, H. (1993). Nature, mass and preferential sites of coarse woody debris deposits in the lower ain valley (Mollon reach), France. *Regulated Rivers: Research & Management*, 8(4):359–372.

Piton, G., Carladous, S., Recking, A., Liebault, F., Tacnet, J., Kuss, D., Quefféléan, Y., and Marco, O. (2017). Why do we build check dams in alpine streams? an historical perspective from the french experience. *Earth Surface Processes and Landforms*, 42(1):91–108.

Piton, G., Horigushi, T., Marchal, L., and Lambert, S. (2020). Open check dams and large wood: head losses and release conditions. *Natural Hazards and Earth System Sciences Discussions*, 2020:1–29.

Piton, G. and Recking, A. (2016). Design of sediment traps with open check dams. ii: woody debris. *Journal of Hydraulic Engineering*, 142(2):04015046.

Rimböck, A. (2004). Design of rope net barriers for woody debris entrapment. introduction of a design concept. In *International Symposium Interpraevent*, pages 265–276.

Rimböck, A. and Strobl, T. (2002). Loads on rope net constructions for woody debris entrapment in torrents. In *International Congress "Interpraevent*, pages 797–807.

Roni, P., Beechie, T., Pess, G., and Hanson, K. (2014). Wood placement in river restoration: fact, fiction, and future direction. *Canadian Journal of Fisheries and Aquatic Sciences*, 72(3):466–478.

Rossi, G. and Armanini, A. (2020). Experimental analysis of open check dams and protection bars against debris flows and driftwood. *Environmental Fluid Mechanics*, 20(3):559–578.

Roth, A., Wendeler, C., and Amend, F. (2010). Use of properly designed flexible barriers to mitigate debris flow natural hazards. In *GeoFlorida 2010: Advances in Analysis, Modeling & Design*, pages 3207–3216.

Ruiz-Villanueva, V., Mazzorana, B., Bladé, E., Bürkli, L., Iribarren-Anacona, P., Mao, L., Nakamura, F., Ravazzolo, D., Rickenmann, D., Sanz-Ramos, M., et al. (2019). Characterization of wood-laden flows in rivers. *Earth Surface Processes and Landforms*, 44(9):1694–1709.

Ruiz-Villanueva, V., Piégay, H., Gaertner, V., Perret, F., and Stoffel, M. (2016a). Wood density and moisture sorption and its influence on large wood mobility in rivers. *Catena*, 140:182–194.

Ruiz-Villanueva, V., Piégay, H., Gurnell, A. M., Marston, R. A., and Stoffel, M. (2016b). Recent advances quantifying the large wood dynamics in river basins: New methods and remaining challenges: Large Wood Dynamics. *Reviews of Geophysics*, 54(3):611–652.

Sawyer, A. H. and Cardenas, M. B. (2012). Effect of experimental wood addition on hyporheic exchange and thermal dynamics in a losing meadow stream. *Water Resources Research*, 48(10).

Schalko, I. (2018). *Modeling Hazards Related to Large Wood in Rivers*. Doctoral Thesis, ETH Zurich.

Schalko, I., Lageder, C., Schmocker, L., Weitbrecht, V., and Boes, R. (2019a). Laboratory flume experiments on the formation of spanwise large wood accumulations part i: Effect on backwater rise. *Water Resources Research*.

Schalko, I., Lageder, C., Schmocker, L., Weitbrecht, V., and Boes, R. (2019b). Laboratory flume experiments on the formation of spanwise large wood accumulations part II: Effect on local scour. *Water Resources Research*.

Schmocker, L. and Hager, W. H. (2013). Scale modeling of wooden debris accumulation at a debris rack. *Journal of Hydraulic Engineering*, 139(8):827–836.

Sheridan, W. L. (1969). *Effects of log debris jams on salmon spawning riffles in Saginaw Creek*. US Forest Service, Alaska Region.

Shields, F. D., Knight, S. S., and Stofleth, J. M. (2008). Stream bed organic carbon and biotic integrity. *Aquatic Conservation: Marine and Freshwater Ecosystems*, 18(5):761–779.

Volkwein, A. (2014). *Flexible debris flow barriers: Design and application*. Swiss Federal Institute for Forest, Snow and Landscape Research WSL.

Ward, G. M. and Aumen, N. G. (1986). Woody Debris as a Source of Fine Particulate Organic Matter in Coniferous Forest Stream Ecosystems. *Canadian Journal of Fisheries and Aquatic Sciences*, 43(8):1635–1642.

Wendeler, C. (2016). Debris-flow protection systems for mountain torrents. *WSL Berichte. Swiss Federal Institute for Forest, Snow and Landscape Research WSL*.

Wendeler, C., Volkwein, A., Roth, A., Denk, M., and Wartmann, S. (2007). Field measurements and numerical modelling of flexible debris flow barriers. *Debris-Flow Hazards Mitig. Mech. Predict. Assess. Millpress, Rotterdam*, pages 681–687.

Wohl, E., Bledsoe, B. P., Fausch, K. D., Kramer, N., Bestgen, K. R., and Gooseff, M. N. (2016). Management of Large Wood in Streams: An Overview and Proposed Framework for Hazard Evaluation. *JAWRA Journal of the American Water Resources Association*, 52(2):315–335.

Appendices

Appendix A

Design of the flexible barrier according to Rimböck (2004)

- **Calculation of the height of the Net in the model**

  The data in the model, correspond to the lengths, discharges, velocities, volumes and Young modulus, used for this research. This appendix was prepared in order to check the equations proposed by Rimböck (2004) and to demonstrate their usefulness in the design of flexible barriers.

  Table A.1 summarizes the elements that were provided in Chapter 3 and that are necessary for the design of the net height, based on the equations described in Chapter 2.

TABLE A.1. Data for design of the flexible barrier.

	Discharge Q (m^3/s)	Velocity U (m/s)	Volume of LW V_s (m^3)	Width b_B (m)	Width b_C (m)	Young Modulus E (GPa)
Model, M	$1 \cdot 10^{-3} - 7.6 \cdot 10^{-3}$	$0.05 - 0.5$	$2 \cdot 10^{-3}$	0.28	0.40	$2.5 - 4.0$
Scale ratio	$\lambda^{5/2}$	$\lambda^{1/2}$	λ^3	λ	λ	λ
Prototype, P	$10 - 76$	$0.2 - 2$	512	11.2	16	$100 - 160$

The unit discharge is given by $q = Q/b_B$, then at the Prototype:

$$q_P = \frac{10}{11.2} = 0.9m^2/s,\ q_P = \frac{76}{11.2} = 6.8m^2/s$$

For the model, the maximum solid volume of large wood planned to be used with a density equal to $\rho_w = 700$ kg/m^3, is approximately $V_{LW} = 2 \cdot 10^{-3}m^3$. To compute the jam volume which is largely permeable, it is required to multiply by a factor due to the porosity equal to 4 (varying in the range 3-5 according to Schalko et al., 2019a), so:

$$V_s = 2 \cdot 10^{-3} * (40)^3 = 128m^3$$

$$V_{LW}{=}\mathrm{a}V_s{=}(4)(128){=}512\mathrm{m}^3$$

So the specific volume of LW is:

$$\frac{V_s}{b_C} = \frac{128}{16} = 8m^3/m$$

According to table 2.1, the maximum discharge exceed the limits that have been established as a reference for the design of a flexible barrier. It means that if we feed the net with the maximum pump discharge, the barrier is supposed to be overloaded according to Rimböck (2004).

In the following, we designed the barrier strictly according to Rimböck (2004) and made it low enough to explore its overloading. It was thus decided to use unit discharge lower than the maximum provided in table 2.1, i.e. $q = 1.8m^3/sm$ which is $Q = 20m^3/s$. We hypothesize a LW volume of $8m^3/m$ which is also lower than the maximum value for this discharge showed in figure 2.4, i.e., approximately $V_{LW}/b_B = 30m^3/m$.

Table A.1, summarizes the results of the calculations made in strict application of Rimböck (2004) guidelines and contains all the values necessary for the calculation of the water depth for this investigation. The first line is representative of the net that will be used. The second line is the maximum loading we can apply with the pump available. Since it results in a net height much higher than the previous line, we expect the net to be overloaded, i.e., overtoped when the pumps reach their maximum capacity. For the fine material, FM, this value was determined using the recommendations of Schalko (2018), while for the roughness, K_{St}, the value given by Rimböck (2004) in his research mentioned above was filled with pure water experiments.

The table A.1 shows the parameters necessaries for the design of the flexible barrier:

Table A.2. Data for determining the water height according to Rimböck (2004)

Channel width b (m)	Unit Discharge q (m^3/sm)	Amount of LW V_{LW}/b_B (m^3/m)	Fine Material FM (%)	Roughness K_{St} ($m^{1/3}$/s)	Water depth (m)
11.2	1.8	8	20	30	4
11.2	6.8	8	20	30	7.7

With all these data it is possible to apply the Equation (2.11) for the calculation of the water depth. Since the $S_0 = 2\%$, an interpolation between $1\%-3\%$ was made, obtaining then $c = 0.225$. Substituting:

Assuming, we design the elevation at water level (freeboard=0)

$$z_2 = 4.44 \times 0.20^{0.17} \times (8)^{0.225} \times \left(1 - \frac{35-30}{105}\right) \times \sqrt{\frac{1.8}{3}} = \mathbf{4m} \tag{A.1}$$

(A.2)

And for an extreme event, q=68m^3/ms, the water depth needs to be:

$$z_2 = 4.44 \times 0.20^{0.17} \times (8)^{0.225} \times \left(1 - \frac{35-30}{105}\right) \times \sqrt{\frac{6.8}{3}} = \mathbf{7.7m} \tag{A.3}$$

This $z_2 \approx 4$ m is equivalent to a flexible barrier about 0.10 m high in the flume which was used in this thesis.

Appendix B

Top view of an experiment

This appendix contains some photographs that were captured in one of the experiments that were done. They correspond to the series 4, repetition 2 with a 3cm plastic sheet + fabric and all the mix put on the channel from the beginning .

The photos were taken with a Canon EOS 100D camera, placed in the upper downstream part of the channel. There were some technical issues, so it was not possible to use it in all the experiments.

The photos are an example of the phases described in section 4.1 (Chapter 4), and have the following sequence:

Phase 1.

1. Start of the experiment, Q≈0.2 l/s
2. Few logs against the net, Q≈0.5 l/s
3. End of step 1, Q≈1 l/s
4. End of step 2, Q≈2.5 l/s

   Phase 2.
5. End of step 3, Q≈4 l/s
6. End of step 4, Q≈5.5 l/s
7. End of step 5, Q≈7.65 l/s
8. Step 6 before laying the fabric, Q≈7.65 l/s

   Phase 3.
9. Step 6: Net + Fabric, just before the release. Q≈7.65 l/s
10. Step 6: Net + Fabric, release condition reached. Q≈7.65 l/s
11. Step 6: Net + Fabric, release condition reached. Q≈7.65 l/s
12. End of the experiment. Q≈7.65 l/s

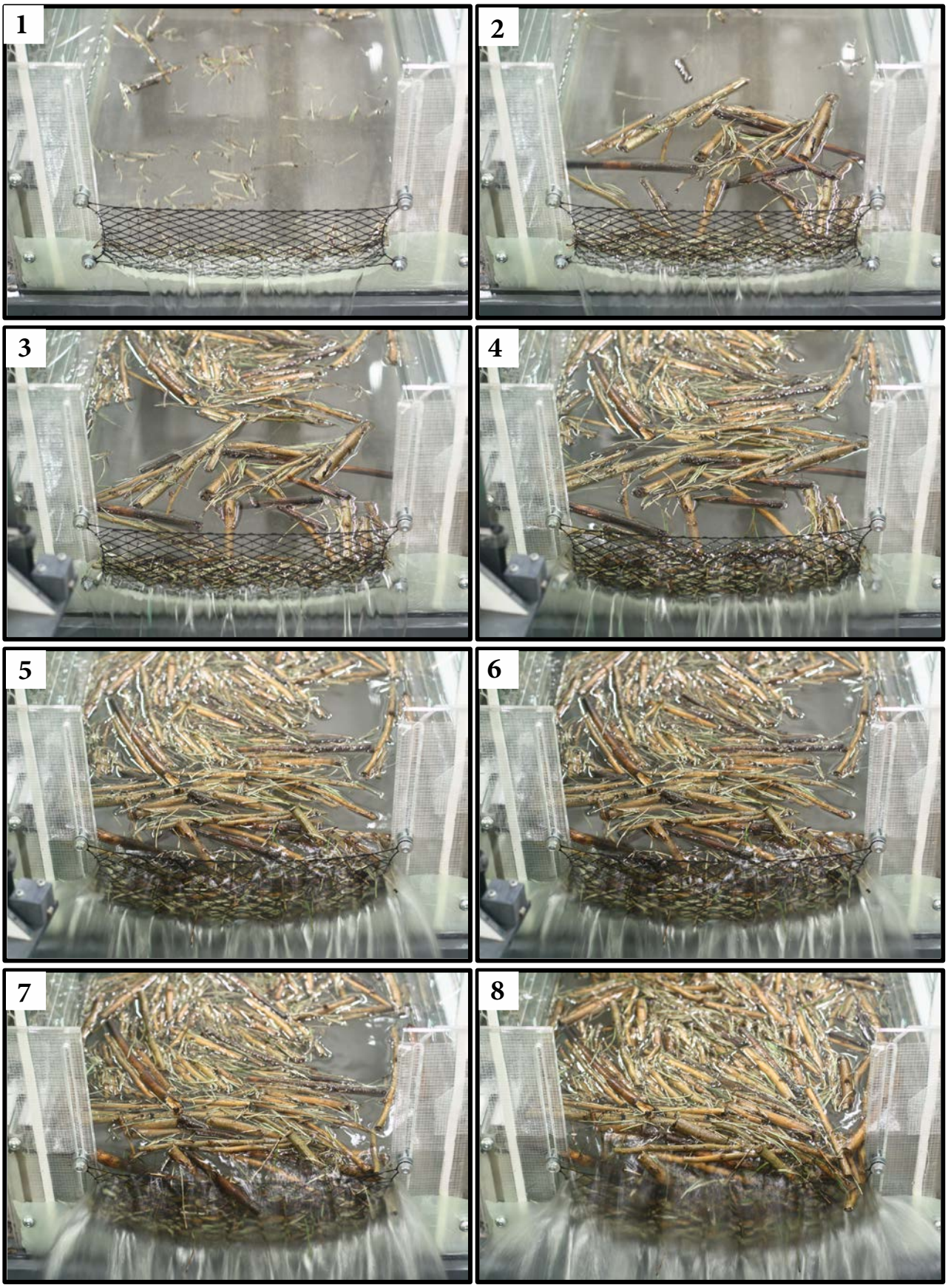

FIGURE B.1. Examples of phases observed in Series 4 repetition 2 with a 3cm plastic sheet + fabric

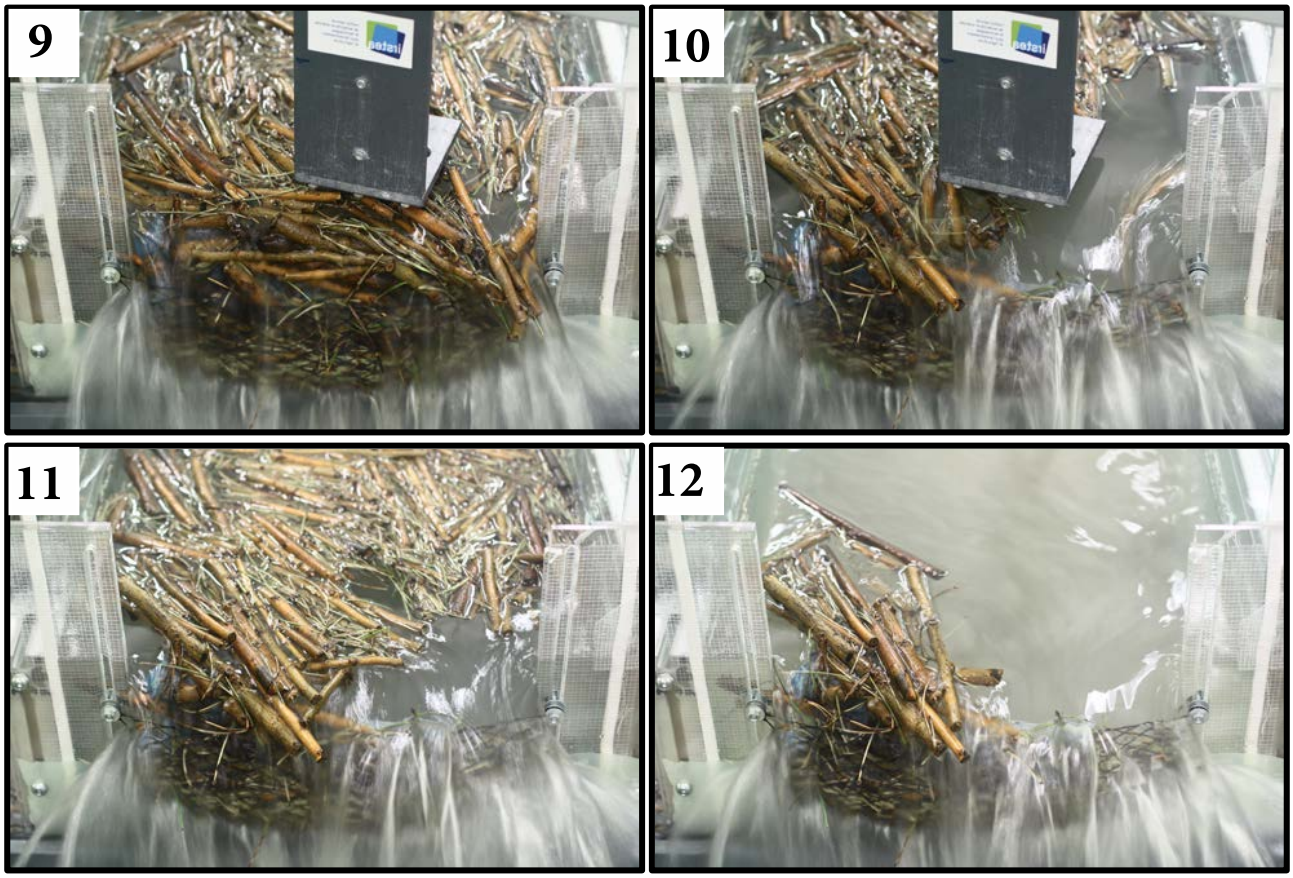

FIGURE B.2. Examples of phases observed in Series 4 repetition 2 with a 3cm plastic sheet + fabric

Appendix C

Full dataset

This appendix is a table with the measurements taken for each of the steps that correspond to the experiments carried out in the laboratory.

For each step the number of Froude, the solid volume of LW in the channel V_s and the variation between the released volume and the total volume of that step (%) were calculated.

SeriesRun	Step	Lcarpet	Q	h	z2	MlwIN	MlwOUT	MassLWin Flume	Vs In Flume	TotalMassL Wwet	MOut/Mtot	Fr	h0	Fr0
#	#	[m]	[l/s]	[m]	[m]	[kg]	[kg]	[kg]	[m3]	[kg]	[%]	[-]	[m]	[-]
Series 1 1-1 (1)	1	0	1,05	0,02	0,086	1,560	0,020	1,56	0,00203	1,78	1%	0,30	12	0,64
Series 1 1-1 (1)	2	0,9	2,02	0,03	0,085	0,000	0,030	1,56	0,00203	1,78	1%	0,31	19	0,64
Series 1 1-1 (1)	3	0,85	3,01	0,038	0,085	0,000	0,040	1,56	0,00203	1,78	1%	0,32	24	0,64
Series 1 1-1 (1)	4	0,8	4,01	0,041	0,084	0,000	0,040	1,56	0,00203	1,78	0%	0,39	29	0,64
Series 1 1-1 (1)	5	0,8	5,02	0,047	0,083	0,000	0,040	1,56	0,00203	1,78	0%	0,39	34	0,64
Series 1 1-1 (1)	6	0,8	6,02	0,052	0,081	0,000	0,040	1,56	0,00203	1,78	0%	0,41	38	0,64
Series 1 1-1 (1)	7	0,7	7,02	0,064	0,081	0,000	0,040	1,56	0,00203	1,78	0%	0,35	43	0,64
Series 1 1-1 (1)	8	0,7	8,02	0,07	0,079	0,000	0,040	1,56	0,00203	1,78	0%	0,35	47	0,64
Series 2 1-1 (1)	1	NA	1,17	0,061	0,080	1,860	0,000	1,86	0,00242	1,86	0%	0,06	61	0,06
Series 2 1-1 (1)	2	NA	1,7	0,071	0,078	0,000	0,000	1,86	0,00242	1,86	0%	0,07	65	0,08
Series 2 1-1 (1)	3	NA	2,1	0,077	0,078	0,000	0,000	1,86	0,00242	1,86	0%	0,08	68	0,09
Series 2 1-1 (1)	4	NA	2,4	0,078	0,072	0,000	0,000	1,86	0,00242	1,86	0%	0,09	70	0,10
Series 2 1-1 (1)	5	NA	2,7	0,072	0,068	0,000	0,000	1,86	0,00242	1,86	0%	0,11	72	0,11
Series 2 1-1 (1)	6	NA	3,01	0,073	0,068	0,000	0,000	1,86	0,00242	1,86	0%	0,12	74	0,12
Series 2 1-1 (1)	7	NA	3,38	0,078	0,068	0,000	0,000	1,86	0,00242	1,86	0%	0,12	77	0,13
Series 2 1-1 (1)	8	NA	3,74	0,082	0,067	0,000	0,000	1,86	0,00242	1,86	0%	0,13	79	0,13
Series 2 1-1 (1)	9	NA	4,05	0,086	0,067	0,000	0,000	1,86	0,00242	1,86	0%	0,13	81	0,14
Series 2 1-1 (1)	10	NA	4,35	0,086	0,066	0,000	0,000	1,86	0,00242	1,86	0%	0,14	83	0,15
Series 2 1-1 (1)	11	NA	4,6	0,085	0,066	0,000	0,040	1,86	0,00242	1,86	2%	0,15	84	0,15
Series 2 1-1 (1)	12	NA	5,05	0,088	0,063	0,000	0,050	1,86	0,00242	1,86	1%	0,15	86	0,16
Series 2 1-1 (1)	13	NA	5,34	0,09	0,063	0,000	0,050	1,86	0,00242	1,86	0%	0,16	88	0,16
Series 2 1-1 (1)	14	NA	5,6	0,095	0,057	0,000	0,080	1,86	0,00242	1,86	2%	0,15	89	0,17
Series 2 1-1 (1)	15	NA	5,84	0,096	0,056	0,000	0,080	1,86	0,00242	1,86	0%	0,16	91	0,17
Series 2 1-1 (1)	16	NA	6,07	0,096	0,056	0,000	0,080	1,86	0,00242	1,86	0%	0,16	92	0,17
Series 2 1-1 (1)	17	NA	6,27	0,095	0,056	0,000	0,080	1,86	0,00242	1,86	0%	0,17	93	0,18
Series 2 1-1 (1)	18	NA	6,44	0,092	0,060	0,000	0,140	1,86	0,00242	1,86	3%	0,18	94	0,18
Series 2 1-1 (1)	19	NA	6,62	0,09	0,060	0,000	0,140	1,86	0,00242	1,86	0%	0,20	95	0,18
Series 2 1-1 (1)	20	NA	6,82	0,09	0,060	0,000	0,160	1,86	0,00242	1,86	1%	0,20	96	0,18
Series 3 1-1 (1)	1	NA	1,15	0,028	0,082	2,040	0,010	2,04	0,00265	2,04	0%	0,20	18	0,39
Series 3 1-1 (1)	2	NA	2,12	0,036	0,081	0,000	0,090	2,04	0,00265	2,04	4%	0,25	26	0,39
Series 3 1-1 (1)	3	NA	3,01	0,042	0,074	0,000	0,120	2,04	0,00265	2,04	1%	0,28	33	0,39
Series 3 1-1 (1)	4	NA	4,06	0,047	0,063	0,000	0,120	2,04	0,00265	2,04	0%	0,32	41	0,39
Series 3 1-1 (1)	5	NA	5,1	0,057	0,062	0,000	0,120	2,04	0,00265	2,04	0%	0,30	48	0,39
Series 3 1-1 (1)	6	NA	6,06	0,065	0,061	0,000	0,120	2,04	0,00265	2,04	0%	0,29	53	0,39
Series 3 1-1 (1)	7	NA	7,03	0,075	0,055	0,000	0,130	2,04	0,00265	2,04	0%	0,27	59	0,39
Series 3 1-1 (1)	8	NA	7,64	0,09	0,045	0,000	0,130	2,04	0,00265	2,04	0%	0,23	62	0,39
Series 3 1-1 (1)	9	NA	7,65	0,12	NA	0,000	0,130	2,04	0,00265	2,04	0%	0,15	62	0,39
Series 3 1-1 (1)	10	NA	7,65	0,125	NA	0,000	0,220	2,04	0,00265	2,04	4%	0,14	62	0,39
Series 4 1-1 (1)	1	2	1,03	0,054	0,082	2,270	0,000	2,27	0,00295	2,06	0%	0,07	46	0,08
Series 4 1-1 (1)	2	1,6	2,5	0,075	0,081	0,000	0,000	2,27	0,00295	2,06	0%	0,10	58	0,14
Series 4 1-1 (1)	3	1,4	4	0,09	0,080	0,000	0,000	2,27	0,00295	2,06	0%	0,12	68	0,18
Series 4 1-1 (1)	4	1,2	5,5	0,103	0,080	0,000	0,000	2,27	0,00295	2,06	0%	0,13	76	0,21
Series 4 1-1 (1)	5	1	7,65	0,12	0,080	0,000	0,000	2,27	0,00295	2,06	0%	0,15	87	0,24
Series 4 1-1 (1)	Fabric	0,9	7,65	0,133	0,080	0,000	2,060	2,27	0,00295	2,06	100%	0,13	87	0,24
Series 1 1-1 (2)	1	1	1,05	0,022	0,086	1,780	0,050	1,78	0,00231	1,78	3%	0,26	12	0,64
Series 1 1-1 (2)	2	0,9	2,02	0,035	0,084	0,000	0,060	1,78	0,00231	1,78	1%	0,25	19	0,64
Series 1 1-1 (2)	3	0,87	3,03	0,038	0,083	0,000	0,060	1,78	0,00231	1,78	0%	0,33	24	0,64
Series 1 1-1 (2)	4	0,87	4,02	0,044	0,082	0,000	0,060	1,78	0,00231	1,78	0%	0,35	29	0,64
Series 1 1-1 (2)	5	0,8	5,15	0,051	0,082	0,000	0,060	1,78	0,00231	1,78	0%	0,36	35	0,64
Series 1 1-1 (2)	6	0,8	6,13	0,055	0,080	0,000	0,060	1,78	0,00231	1,78	0%	0,38	39	0,64
Series 1 1-1 (2)	7	0,8	7,02	0,063	0,080	0,000	0,060	1,78	0,00231	1,78	0%	0,35	43	0,64
Series 1 1-1 (2)	8	0,8	8,01	0,07	0,080	0,000	0,060	1,78	0,00231	1,78	0%	0,35	47	0,64
Series 2 1-1 (2)	1	NA	0,8	0,042	0,078	2,000	0,000	2	0,00260	1,86	0%	0,07	57	0,05

SeriesRun	Step	Lcarpet	Q	h	z2	MlwIN	MlwOUT	MassLWin Flume	Vs In Flume	TotalMassL Wwet	MOut/Mtot	Fr	h0	Fr0
#	#	[m]	[l/s]	[m]	[m]	[kg]	[kg]	[kg]	[m3]	[kg]	[%]	[-]	[m]	[-]
Series 2 1-1 (2)	2	NA	1,32	0,069	0,078	0,000	0,000	2	0,00260	1,86	0%	0,06	62	0,07
Series 2 1-1 (2)	3	NA	1,7	0,075	0,077	0,000	0,000	2	0,00260	1,86	0%	0,07	65	0,08
Series 2 1-1 (2)	4	NA	2,1	0,081	0,077	0,000	0,000	2	0,00260	1,86	0%	0,07	68	0,09
Series 2 1-1 (2)	5	NA	2,4	0,084	0,077	0,000	0,000	2	0,00260	1,86	0%	0,08	70	0,10
Series 2 1-1 (2)	6	NA	2,7	0,084	0,077	0,000	0,000	2	0,00260	1,86	0%	0,09	72	0,11
Series 2 1-1 (2)	7	NA	3,05	0,085	0,077	0,000	0,000	2	0,00260	1,86	0%	0,10	75	0,12
Series 2 1-1 (2)	8	NA	3,4	0,091	0,077	0,000	0,030	2	0,00260	1,86	2%	0,10	77	0,13
Series 2 1-1 (2)	9	NA	3,75	0,092	0,075	0,000	0,070	2	0,00260	1,86	2%	0,11	79	0,13
Series 2 1-1 (2)	10	NA	4,25	0,098	0,073	0,000	0,200	2	0,00260	1,86	7%	0,11	82	0,14
Series 2 1-1 (2)	11	NA	4,77	0,099	0,075	0,000	0,210	2	0,00260	1,86	1%	0,12	85	0,15
Series 2 1-1 (2)	12	NA	5,17	0,104	0,060	0,000	1,860	2	0,00260	1,86	89%	0,12	87	0,16
Series 4 1-1 (2)	1	2	1	0,049	0,081	2,220	0,000	2,22	0,00288	2,1	0%	0,07	46	0,08
Series 4 1-1 (2)	2	1,6	2,53	0,07	0,078	0,000	0,000	2,22	0,00288	2,1	0%	0,11	58	0,14
Series 4 1-1 (2)	3	1,4	4	0,089	0,077	0,000	0,000	2,22	0,00288	2,1	0%	0,12	68	0,18
Series 4 1-1 (2)	4	1,2	5,49	0,1	0,077	0,000	0,000	2,22	0,00288	2,1	0%	0,14	76	0,21
Series 4 1-1 (2)	5	1	7,77	0,115	0,077	0,000	0,000	2,22	0,00288	2,1	0%	0,16	87	0,24
Series 4 1-1 (2)	Fabric	0,9	7,77	0,14	0,075	0,000	2,100	2,22	0,00288	2,1	100%	0,12	87	0,24
Series 1 1-1 (3)	1	1	1,02	0,022	0,086	1,800	0,020	1,8	0,00234	1,8	1%	0,25	12	0,64
Series 1 1-1 (3)	2	1	2,01	0,036	0,085	0,000	0,020	1,8	0,00234	1,8	0%	0,23	19	0,64
Series 1 1-1 (3)	3	0,9	3	0,039	0,084	0,000	0,040	1,8	0,00234	1,8	1%	0,31	24	0,64
Series 1 1-1 (3)	4	0,9	4	0,047	0,083	0,000	0,040	1,8	0,00234	1,8	0%	0,31	29	0,64
Series 1 1-1 (3)	5	0,87	5,07	0,056	0,082	0,000	0,040	1,8	0,00234	1,8	0%	0,31	34	0,64
Series 1 1-1 (3)	6	0,8	6,04	0,06	0,081	0,000	0,040	1,8	0,00234	1,8	0%	0,33	39	0,64
Series 1 1-1 (3)	7	0,8	7,02	0,064	0,081	0,000	0,040	1,8	0,00234	1,8	0%	0,35	43	0,64
Series 1 1-1 (3)	8	0,8	8	0,068	0,081	0,000	0,040	1,8	0,00234	1,8	0%	0,36	47	0,64
Series 2 1-1 (3)	1	NA	1,03	0,03	0,063	2,000	0,000	2	0,00260	2	0%	0,16	59	0,06
Series 2 1-1 (3)	2	NA	2,1	0,062	0,062	0,000	0,000	2	0,00260	2	0%	0,11	68	0,09
Series 2 1-1 (3)	3	NA	3,03	0,07	0,063	0,000	0,000	2	0,00260	2	0%	0,13	74	0,12
Series 2 1-1 (3)	4	NA	4,1	0,08	0,063	0,000	0,010	2	0,00260	2	1%	0,14	81	0,14
Series 2 1-1 (3)	5	NA	5,15	0,085	0,063	0,000	0,060	2	0,00260	2	3%	0,17	87	0,16
Series 2 1-1 (3)	6	NA	6,12	0,1	0,063	0,000	1,350	2	0,00260	2	65%	0,15	92	0,17
Series 4 1-1 (3)	1	1,7	1,16	0,056	0,081	2,420	0,000	2,42	0,00314	2,18	0%	0,07	48	0,09
Series 4 1-1 (3)	2	1,5	2,55	0,075	0,080	0,000	0,000	2,42	0,00314	2,18	0%	0,10	58	0,14
Series 4 1-1 (3)	3	1,2	4	0,097	0,080	0,000	0,000	2,42	0,00314	2,18	0%	0,11	68	0,18
Series 4 1-1 (3)	4	1,1	5,5	0,1075	0,080	0,000	0,010	2,42	0,00314	2,18	0%	0,12	76	0,21
Series 4 1-1 (3)	5	1	7,8	0,125	0,080	0,000	0,020	2,42	0,00314	2,18	0%	0,14	87	0,24
Series 4 1-1 (3)	Fabric	0,9	7,8	0,145	0,074	0,000	2,180	2,42	0,00314	2,18	99%	0,11	87	0,24
Series 1 1-3 (1)	1	0,3	1,03	0,017	0,086	0,603	0,020	0,603	0,00078	1,81	1%	0,37	12	0,64
Series 1 1-3 (1)	2	0,8	2,03	0,026	0,085	0,603	0,040	1,206	0,00157	1,81	1%	0,39	19	0,64
Series 1 1-3 (1)	3	1,2	3	0,039	0,084	0,603	0,040	1,809	0,00235	1,81	0%	0,31	24	0,64
Series 1 1-3 (1)	4	1,2	4	0,043	0,084	0,000	0,040	1,809	0,00235	1,81	0%	0,36	29	0,64
Series 1 1-3 (1)	5	1,1	5	0,053	0,083	0,000	0,050	1,809	0,00235	1,81	1%	0,33	34	0,64
Series 1 1-3 (1)	6	1,1	6,01	0,07	0,081	0,000	0,050	1,809	0,00235	1,81	0%	0,26	38	0,64
Series 1 1-3 (1)	7	1	7,06	0,078	0,081	0,000	0,050	1,809	0,00235	1,81	0%	0,26	43	0,64
Series 1 1-3 (1)	8	1	7,84	0,084	0,080	0,000	0,050	1,809	0,00235	1,81	0%	0,26	46	0,64
Series 3 1-3 (1)	1	NA	1	0,044	0,061	0,000	0,000	0	0,00000	2	0%	0,09	16	0,39
Series 3 1-3 (1)	2	NA	2,1	0,06	0,061	0,670	0,000	0,67	0,00087	2	0%	0,11	26	0,39
Series 3 1-3 (1)	3	NA	3,03	0,072	0,061	0,670	0,000	1,34	0,00174	2	0%	0,13	34	0,39
Series 3 1-3 (1)	4	NA	4,13	0,079	0,050	0,670	0,100	2,01	0,00261	2	5%	0,15	41	0,39
Series 3 1-3 (1)	5	NA	5,18	0,09	0,060	0,000	1,780	2,01	0,00261	2	84%	0,15	48	0,39
Series 1 1-3 (2)	1	0,3	1,13	0,014	0,086	0,603	0,030	0,603	0,00078	1,8	2%	0,54	13	0,64
Series 1 1-3 (2)	2	0,95	2,05	0,031	0,086	0,603	0,030	1,206	0,00157	1,8	0%	0,30	19	0,64
Series 1 1-3 (2)	3	1,1	3	0,036	0,084	0,603	0,030	1,809	0,00235	1,8	0%	0,35	24	0,64
Series 1 1-3 (2)	4	1,1	4,09	0,06	0,084	0,000	0,030	1,809	0,00235	1,8	0%	0,22	30	0,64
Series 1 1-3 (2)	5	1	5,1	0,074	0,083	0,000	0,030	1,809	0,00235	1,8	0%	0,20	34	0,64

SeriesRun	Step	Lcarpet	Q	h	z2	MlwIN	MlwOUT	MassLWin Flume	Vs In Flume	TotalMassL Wwet	MOut/Mtot	Fr	h0	Fr0
#	#	[m]	[l/s]	[m]	[m]	[kg]	[kg]	[kg]	[m3]	[kg]	[%]	[-]	[m]	[-]
Series 1 1-3 (2)	6	1	6,1	0,084	0,082	0,000	0,030	1,809	0,00235	1,8	0%	0,20	39	0,64
Series 1 1-3 (2)	7	0,9	7	0,09	0,082	0,000	0,030	1,809	0,00235	1,8	0%	0,21	43	0,64
Series 1 1-3 (2)	8	0,9	7,8	0,093	0,077	0,000	0,030	1,809	0,00235	1,8	0%	0,22	46	0,64
Series 3 1-3 (2)	1	NA	1	0,057	0,078	0,000	0,000	0	0,00000	2	NA	0,06	16	0,39
Series 3 1-3 (2)	2	NA	2,1	0,07	0,072	0,670	0,000	0,67	0,00087	2	NA	0,09	26	0,39
Series 3 1-3 (2)	3	NA	3,05	0,076	0,072	0,670	0,000	1,34	0,00174	2	NA	0,12	34	0,39
Series 3 1-3 (2)	4	NA	4,16	0,087	0,072	0,670	0,000	2,01	0,00261	2	NA	0,13	41	0,39
Series 3 1-3 (2)	5	NA	4,5	0,095	0,072	0,000	0,010	2,01	0,00261	2	NA	0,12	44	0,39
Series 3 1-3 (2)	6	NA	5,15	0,095	0,072	0,000	0,120	2,01	0,00261	2	NA	0,14	48	0,39
Series 3 1-3 (2)	7	NA	5,5	0,1	0,072	0,000	0,140	2,01	0,00261	2	NA	0,14	50	0,39
Series 3 1-3 (2)	8	NA	6,15	0,105	0,070	0,000	1,560	2,01	0,00261	2	NA	0,14	54	0,39
Series 1 1-3 (3)	1	0,3	1,12	0,023	0,087	0,603	0,100	0,603	0,00078	1,8	6%	0,26	13	0,64
Series 1 1-3 (3)	2	0,9	2,03	0,035	0,086	0,603	0,100	1,206	0,00157	1,8	0%	0,25	19	0,64
Series 1 1-3 (3)	3	1	3,05	0,038	0,084	0,603	0,100	1,809	0,00235	1,8	0%	0,33	24	0,64
Series 1 1-3 (3)	4	1	4,1	0,043	0,084	0,000	0,100	1,809	0,00235	1,8	0%	0,37	30	0,64
Series 1 1-3 (3)	5	0,9	5,05	0,053	0,082	0,000	0,100	1,809	0,00235	1,8	0%	0,33	34	0,64
Series 1 1-3 (3)	6	0,9	6,06	0,062	0,081	0,000	0,100	1,809	0,00235	1,8	0%	0,31	39	0,64
Series 1 1-3 (3)	7	0,9	7,02	0,068	0,080	0,000	0,100	1,809	0,00235	1,8	0%	0,32	43	0,64
Series 1 1-3 (3)	8	0,8	7,82	0,074	0,079	0,000	0,100	1,809	0,00235	1,8	0%	0,31	46	0,64
Series 3 1-3 (3)	1	NA	1	0,057	0,078	0,000	0,000	0	0,00000	1,72	0%	0,06	16	0,39
Series 3 1-3 (3)	2	NA	2,1	0,075	0,077	0,670	0,000	0,67	0,00087	1,72	0%	0,08	26	0,39
Series 3 1-3 (3)	3	NA	3,05	0,093	0,077	0,670	0,000	1,34	0,00174	1,72	0%	0,09	34	0,39
Series 3 1-3 (3)	4	NA	4,13	0,1	0,077	0,670	0,130	2,01	0,00261	1,72	8%	0,10	41	0,39
Series 3 1-3 (3)	5	NA	4,73	0,103	0,082	0,000	1,720	2,01	0,00261	1,72	92%	0,11	45	0,39
Series 1 1-6 (1)	1	0,09	1	0,027	0,085	0,300	0,030	0,3	0,00039	1,8	2%	0,18	12	0,64
Series 1 1-6 (1)	2	0,5	2,07	0,045	0,083	0,300	0,030	0,6	0,00078	1,8	0%	0,17	19	0,64
Series 1 1-6 (1)	3	0,7	3	0,048	0,083	0,300	0,030	0,9	0,00117	1,8	0%	0,23	24	0,64
Series 1 1-6 (1)	4	0,9	4	0,049	0,081	0,300	0,030	1,2	0,00156	1,8	0%	0,29	29	0,64
Series 1 1-6 (1)	5	1	5,01	0,056	0,081	0,300	0,030	1,5	0,00195	1,8	0%	0,30	34	0,64
Series 1 1-6 (1)	6	1,1	6	0,07	0,079	0,300	0,030	1,8	0,00234	1,8	0%	0,26	38	0,64
Series 1 1-6 (1)	7	1,1	6,95	0,077	0,077	0,000	0,030	1,8	0,00234	1,8	0%	0,26	42	0,64
Series 1 1-6 (1)	8	1,1	7,9	0,082	0,075	0,000	0,030	1,8	0,00234	1,8	0%	0,27	46	0,64
Series 1 1-6 (2)	1	0,1	1,17	0,018	0,085	0,317	0,040	0,316667	0,00041	1,9	2%	0,39	13	0,64
Series 1 1-6 (2)	2	0,4	2	0,029	0,084	0,317	0,070	0,633333	0,00082	1,9	2%	0,32	18	0,64
Series 1 1-6 (2)	3	0,6	3,03	0,036	0,083	0,317	0,070	0,95	0,00123	1,9	0%	0,35	24	0,64
Series 1 1-6 (2)	4	0,8	4	0,043	0,081	0,317	0,070	1,266667	0,00165	1,9	0%	0,36	29	0,64
Series 1 1-6 (2)	5	0,9	4,95	0,058	0,080	0,317	0,070	1,583333	0,00206	1,9	0%	0,28	34	0,64
Series 1 1-6 (2)	6	1	6	0,067	0,079	0,317	0,070	1,9	0,00247	1,9	0%	0,28	38	0,64
Series 1 1-6 (2)	7	1	6,96	0,077	0,078	0,000	0,070	1,9	0,00247	1,9	0%	0,26	42	0,64
Series 1 1-6 (2)	8	1	8,51	0,075	0,078	0,000	0,070	1,9	0,00247	1,9	0%	0,33	48	0,64
Series 1 1-6 (3)	1	0,1	1,07	0,026	0,086	0,300	0,050	0,3	0,00039	1,8	3%	0,20	12	0,64
Series 1 1-6 (3)	2	0,4	2,18	0,028	0,085	0,300	0,090	0,6	0,00078	1,8	2%	0,37	20	0,64
Series 1 1-6 (3)	3	0,6	3,1	0,048	0,083	0,300	0,090	0,9	0,00117	1,8	0%	0,24	25	0,64
Series 1 1-6 (3)	4	0,8	4,15	0,055	0,082	0,300	0,090	1,2	0,00156	1,8	0%	0,26	30	0,64
Series 1 1-6 (3)	5	1	5,2	0,071	0,080	0,300	0,090	1,5	0,00195	1,8	0%	0,22	35	0,64
Series 1 1-6 (3)	6	1,1	6,28	0,082	0,078	0,300	0,090	1,8	0,00234	1,8	0%	0,21	40	0,64
Series 1 1-6 (3)	7	1,1	7,1	0,088	0,079	0,000	0,090	1,8	0,00234	1,8	0%	0,22	43	0,64
Series 1 1-6 (3)	8	1,1	7,8	0,085	0,076	0,000	0,090	1,8	0,00234	1,8	0%	0,25	46	0,64
Series 1 1-7 (1)	1	0,08	1,04	0,017	0,085	0,247	0,090	0,247143	0,00032	1,73	5%	0,37	12	0,64
Series 1 1-7 (1)	2	0,4	2,14	0,025	0,085	0,247	0,090	0,494286	0,00064	1,73	0%	0,43	19	0,64
Series 1 1-7 (1)	3	0,5	3,06	0,04	0,083	0,247	0,090	0,741429	0,00096	1,73	0%	0,31	25	0,64
Series 1 1-7 (1)	4	0,7	4,13	0,05	0,081	0,247	0,090	0,988571	0,00128	1,73	0%	0,29	30	0,64
Series 1 1-7 (1)	5	0,8	5,15	0,062	0,080	0,247	0,090	1,235714	0,00160	1,73	0%	0,27	35	0,64
Series 1 1-7 (1)	6	0,9	6,23	0,07	0,080	0,247	0,090	1,482857	0,00193	1,73	0%	0,27	39	0,64
Series 1 1-7 (1)	7	1	7,04	0,08	0,080	0,000	0,090	1,482857	0,00193	1,73	0%	0,25	43	0,64

SeriesRun	Step	Lcarpet	Q	h	z2	MlwIN	MlwOUT	MassLWin Flume	Vs In Flume	TotalMassL Wwet	MOut/Mtot	Fr	h0	Fr0
#	#	[m]	[l/s]	[m]	[m]	[kg]	[kg]	[kg]	[m3]	[kg]	[%]	[-]	[m]	[-]
Series 1 1-7 (1)	8	1,1	7,7	0,085	0,075	0,000	0,090	1,482857	0,00193	1,73	0%	0,25	45	0,64
Series 1 1-7 (2)	1	-	0,99	0,017	0,087	0,276	0,160	0,275714	0,00036	1,93	8%	0,36	12	0,64
Series 1 1-7 (2)	2	0,2	2	0,029	0,085	0,276	0,230	0,551429	0,00072	1,93	4%	0,32	18	0,64
Series 1 1-7 (2)	3	0,4	2,9	0,035	0,084	0,276	0,250	0,827143	0,00107	1,93	1%	0,35	24	0,64
Series 1 1-7 (2)	4	0,6	4,12	0,048	0,082	0,276	0,250	1,102857	0,00143	1,93	0%	0,31	30	0,64
Series 1 1-7 (2)	5	0,6	5,12	0,065	0,080	0,276	0,250	1,378571	0,00179	1,93	0%	0,25	35	0,64
Series 1 1-7 (2)	6	0,7	6,08	0,073	0,078	0,276	0,250	1,654286	0,00215	1,93	0%	0,25	39	0,64
Series 1 1-7 (2)	7	0,8	7,18	0,078	0,078	0,000	0,250	1,654286	0,00215	1,93	0%	0,26	43	0,64
Series 1 1-7 (2)	8	0,9	7,6	0,08	0,075	0,000	0,250	1,654286	0,00215	1,93	0%	0,27	45	0,64
Series 1 1-7 (3)	1	-	1	0,014	0,087	0,271	0,050	0,271429	0,00035	1,9	3%	0,48	12	0,64
Series 1 1-7 (3)	2	0,1	2,11	0,025	0,086	0,271	0,090	0,542857	0,00071	1,9	2%	0,43	19	0,64
Series 1 1-7 (3)	3	0,4	3	0,035	0,085	0,271	0,090	0,814286	0,00106	1,9	0%	0,37	24	0,64
Series 1 1-7 (3)	4	0,5	4,02	0,04	0,080	0,271	0,090	1,085714	0,00141	1,9	0%	0,40	29	0,64
Series 1 1-7 (3)	5	0,6	5,02	0,055	0,080	0,271	0,090	1,357143	0,00176	1,9	0%	0,31	34	0,64
Series 1 1-7 (3)	6	0,7	6,15	0,07	0,078	0,271	0,090	1,628571	0,00212	1,9	0%	0,27	39	0,64
Series 1 1-7 (3)	7	0,8	7,05	0,078	0,078	0,000	0,090	1,628571	0,00212	1,9	0%	0,26	43	0,64
Series 1 1-7 (3)	8	1	7,62	0,079	0,077	0,000	0,090	1,628571	0,00212	1,9	0%	0,27	45	0,64
Series 1 NoWood	1	NA	1,09	0,013	0,085	NA	NA	0	0,00000	0	NA	0,59	12	0,64
Series 1 NoWood	2	NA	2,03	0,016	0,085	NA	NA	0	0,00000	0	NA	0,80	19	0,64
Series 1 NoWood	3	NA	3,01	0,024	0,085	NA	NA	0	0,00000	0	NA	0,65	24	0,64
Series 1 NoWood	4	NA	4,02	0,028	0,084	NA	NA	0	0,00000	0	NA	0,68	29	0,64
Series 1 NoWood	5	NA	5,02	0,032	0,084	NA	NA	0	0,00000	0	NA	0,70	34	0,64
Series 1 NoWood	6	NA	6,02	0,037	0,084	NA	NA	0	0,00000	0	NA	0,68	38	0,64
Series 1 NoWood	7	NA	7,03	0,042	0,084	NA	NA	0	0,00000	0	NA	0,65	43	0,64
Series 1 NoWood	8	NA	8	0,048	0,084	NA	NA	0	0,00000	0	NA	0,61	47	0,64
Series 2 NoWood	1	NA	3,31	0,075	0,078	0,000	0,000	0	0,00000	0	NA	0,13	76	0,13
Series 2 NoWood	2	NA	4,46	0,085	0,078	0,000	0,000	0	0,00000	0	NA	0,14	83	0,15
Series 2 NoWood	3	NA	5,69	0,09	0,080	0,000	0,000	0	0,00000	0	NA	0,17	90	0,17
Series 2 NoWood	4	NA	6,66	0,093	0,076	0,000	0,000	0	0,00000	0	NA	0,19	95	0,18
Series 2 NoWood	5	NA	7,02	0,095	0,077	0,000	0,000	0	0,00000	0	NA	0,19	97	0,19
Series 2 NoWood	6	NA	7,31	0,096	0,077	0,000	0,000	0	0,00000	0	NA	0,20	98	0,19
Series 3 NoWood	1	NA	1,16	0,013	0,083	0,000	0,000	0	0,00000	0	NA	0,62	18	0,39
Series 3 NoWood	2	NA	2,17	0,024	0,083	0,000	0,000	0	0,00000	0	NA	0,47	27	0,39
Series 3 NoWood	3	NA	3,07	0,031	0,082	0,000	0,000	0	0,00000	0	NA	0,45	34	0,39
Series 3 NoWood	4	NA	4,14	0,042	0,081	0,000	0,000	0	0,00000	0	NA	0,38	41	0,39
Series 3 NoWood	5	NA	5,18	0,05	0,080	0,000	0,000	0	0,00000	0	NA	0,37	48	0,39
Series 3 NoWood	6	NA	6,02	0,054	0,079	0,000	0,000	0	0,00000	0	NA	0,38	53	0,39
Series 3 NoWood	7	NA	6,93	0,06	0,079	0,000	0,000	0	0,00000	0	NA	0,38	58	0,39
Series 3 NoWood	8	NA	7,85	0,065	0,079	0,000	0,000	0	0,00000	0	NA	0,38	63	0,39
Series 4 NoWood	1	NA	1,02	0,045	NA	0,000	0,000	0	0,00000	0	NA	0,09	46	0,08
Series 4 NoWood	2	NA	2,02	0,057	NA	0,000	0,000	0	0,00000	0	NA	0,12	55	0,13
Series 4 NoWood	3	NA	3,11	0,064	NA	0,000	0,000	0	0,00000	0	NA	0,15	62	0,16
Series 4 NoWood	4	NA	4	0,07	NA	0,000	0,000	0	0,00000	0	NA	0,17	68	0,18
Series 4 NoWood	5	NA	5,01	0,075	NA	0,000	0,000	0	0,00000	0	NA	0,19	73	0,20
Series 4 NoWood	6	NA	6,09	0,08	NA	NA	0,000	0	0,00000	0	NA	0,21	79	0,22
Series 4 NoWood	7	NA	7	0,083	NA	0,000	0,000	0	0,00000	0	NA	0,23	84	0,23
Series 4 NoWood	8	NA	7,61	0,086	NA	0,000	0,000	0	0,00000	0	NA	0,24	87	0,24

Centre Center Lyon-Grenoble - Auvergne-Rhône-Alpes
2 rue de la Papeterie BP 76,
38 402 St-Martin-d'Hères - France

Rejoignez-nous sur :

https://www.inrae.fr/centres/lyon-grenoble-auvergne-rhone-alpes

INRAE
la science pour la vie, l'humain, la terre